Introduction to geodesy

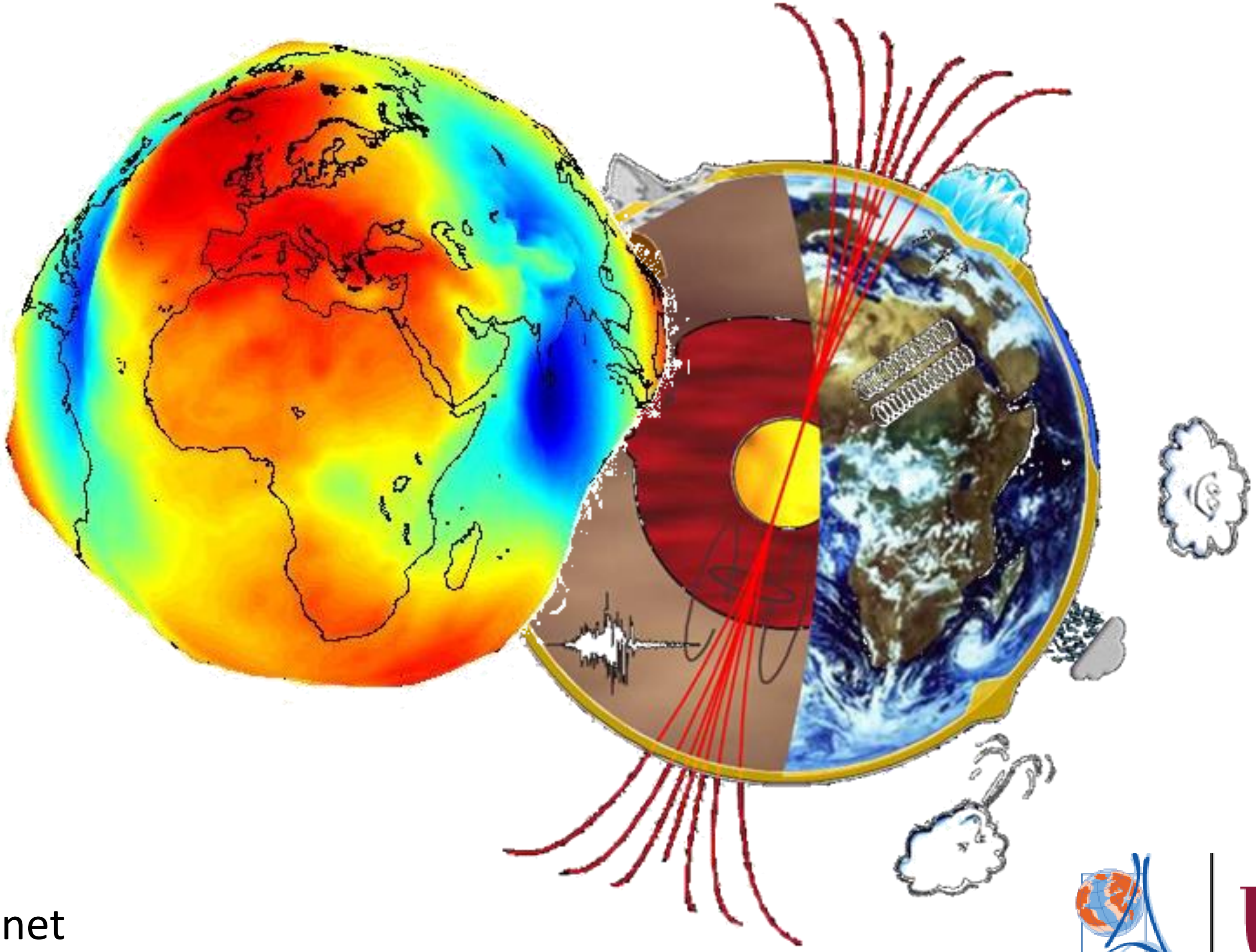

Isabelle Panet
IPGP, IGN, Université de Paris

Introduction to geodesy

1. A very old question: what is the shape of the Earth?

2. The revolution of the satellites

3. Gravity field from a static mass distribution and its spherical harmonics representation

4. Sources of the gravity field (geological timescales)

5. Time-varying gravity and surface displacements (timescales of weeks to secular)

A very old science

Aristotle *4th century BC*

Circular shadow of the Earth on the Moon during lunar eclipses

Ex: lunar eclipse of 03/03/2007

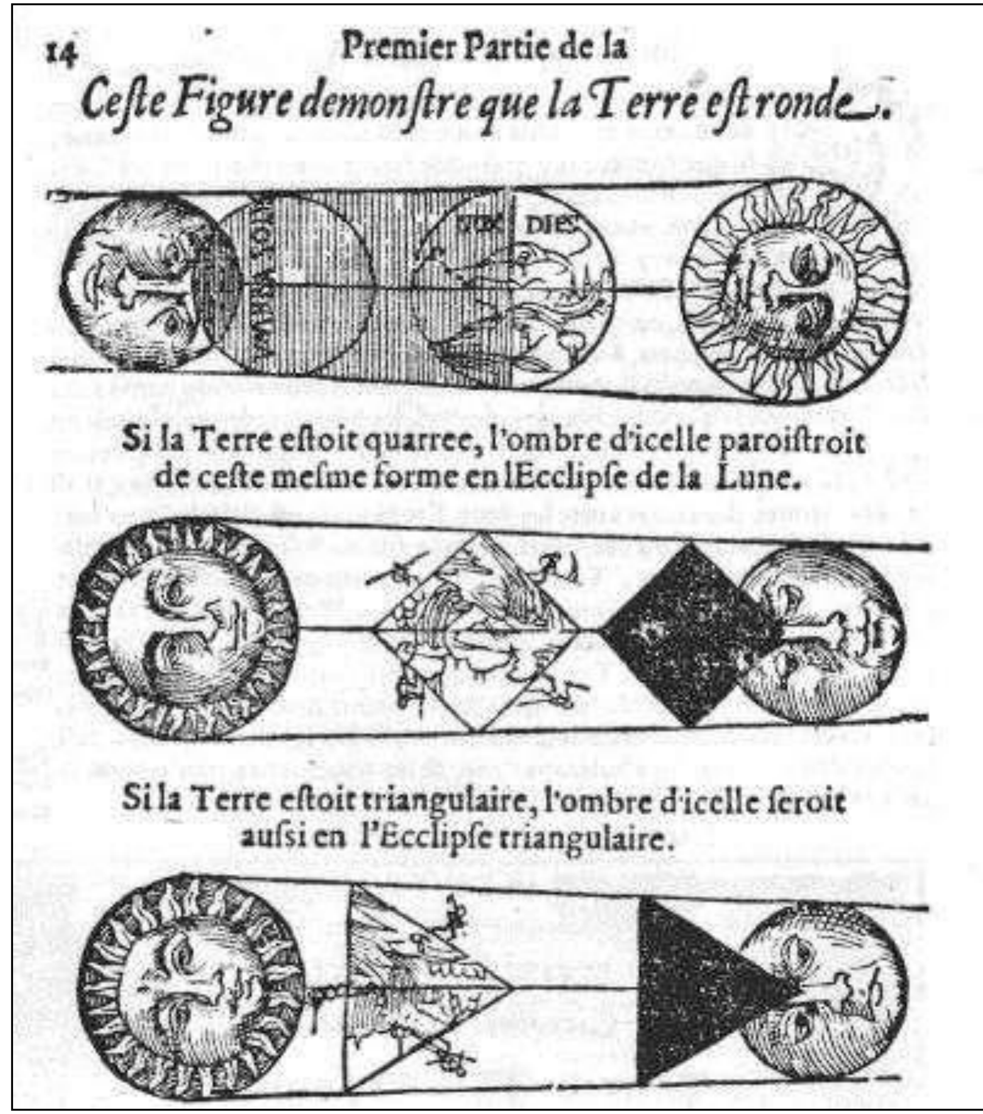

14 Premier Partie de la

Ceſte Figure demonſtre que la Terre eſt ronde.

Si la Terre eſtoit quarree, l'ombre d'icelle paroiſtroit de ceſte meſme forme en l'Ecclipſe de la Lune.

Si la Terre eſtoit triangulaire, l'ombre d'icelle ſeroit auſsi en l'Ecclipſe triangulaire.

Bibliothèque de l'Observatoire de Paris. Inference by Apian, German astronomer, 17th century.

Measuring the Earth's circumference

Eratosthene

3rd century BC

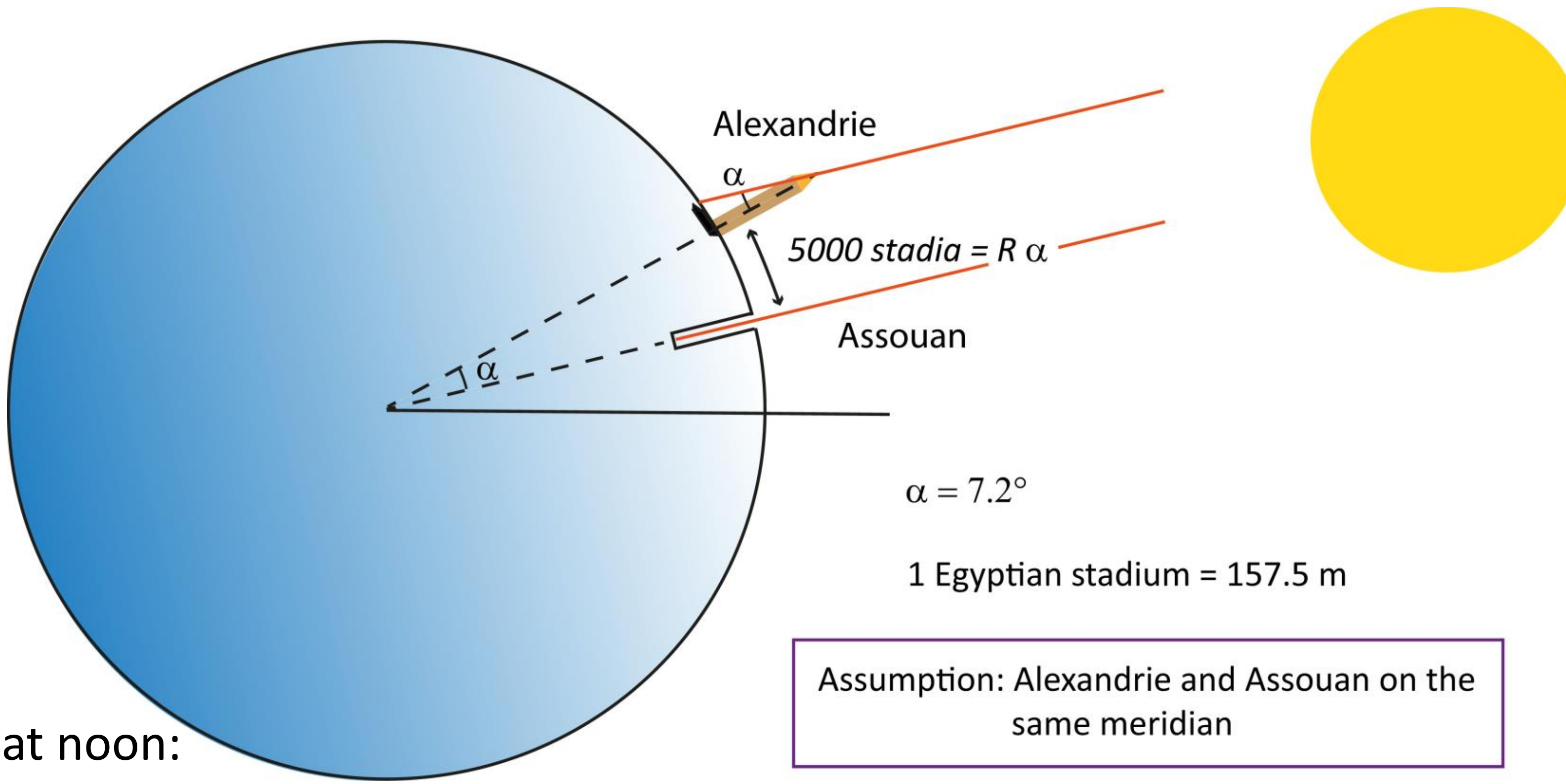

Assumption: Alexandrie and Assouan on the same meridian

Summer solstice at noon:

- no shadow in a well in Assouan
- shadow of an obelisk in Alexandrie

Earth's circumference estimate: 39375 km (instead of 40 008 km along a meridian)

A spheroidal shape

Richer's *Observations astronomiques et physiques faites en l'isle de Caïenne* (Paris, 1679)

Richer (*1672*)

Slower oscillations of the pendulum in Cayenne (near the Equator) than in Paris

$$T = 2\pi\sqrt{\frac{\ell}{g}}$$

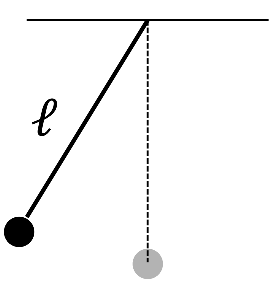

Newton (*1689*)

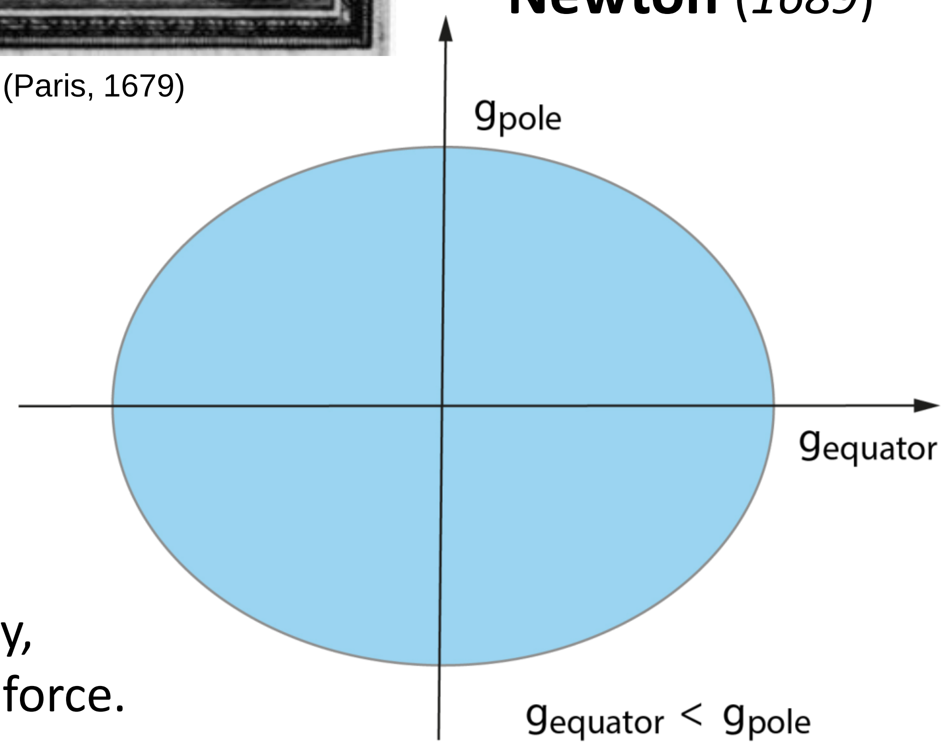

<u>Newton</u>: spheroidal shape of a rotating fluid body, flattened at the poles because of the centrifugal force.

Measuring a meridian arc

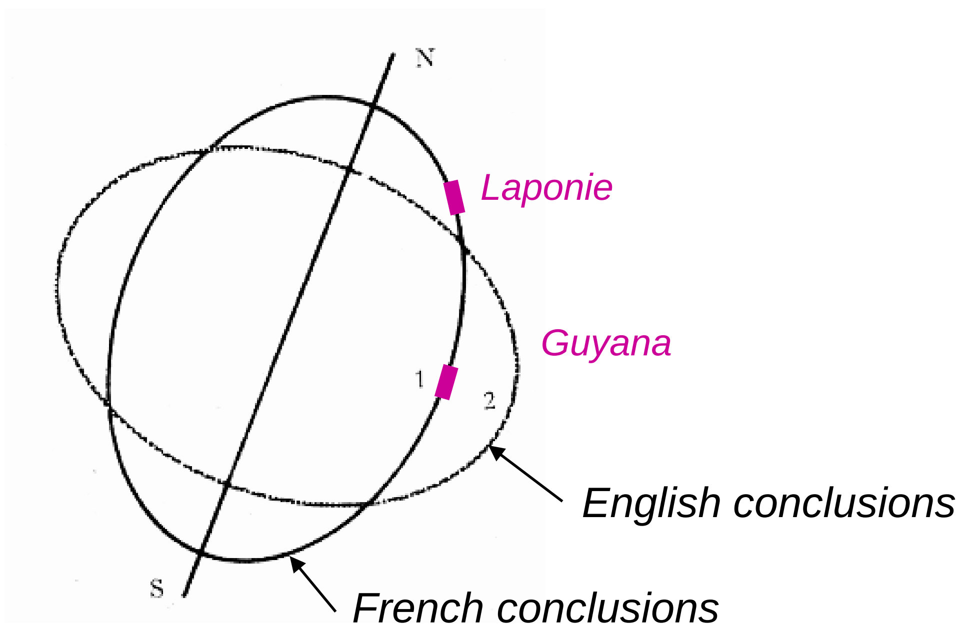

Expeditions to measure a meridian arc near the Equator and near the pole, to discriminate between a prolate or an oblate spheroid

Measurements of long distances from many measurements of shorter distances and angles within a network of points.

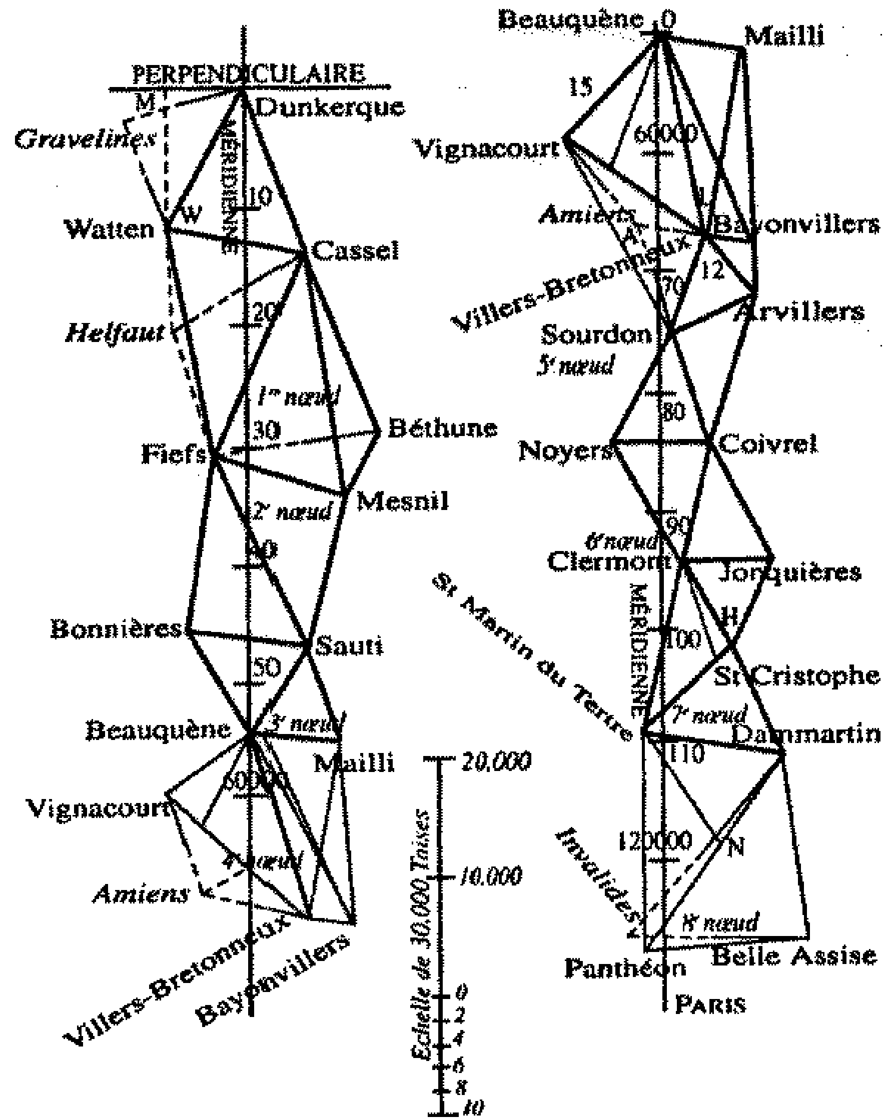

Triangulation of Paris meridian (Dunkerque-Perpignan)

Picard: 1 arc = 108 km (North of France)
110 km (South of France)

Enigmatic deviations of the plumb line

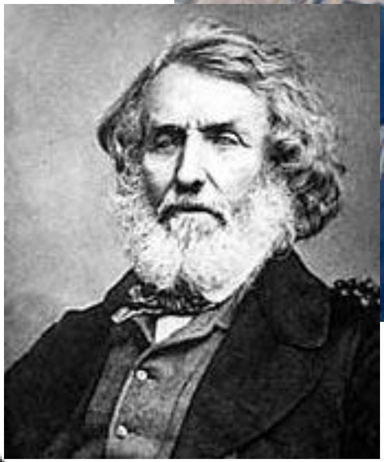

Everest (1790-1866)

- ***Near mountains***

Bouguer (1698-1758)

- ***When measuring meridian arcs***

The local vertical deviates from the normal to the ellipsoid (Laplace, Gauss, Bessel)

The Figure of the Earth: the geoid

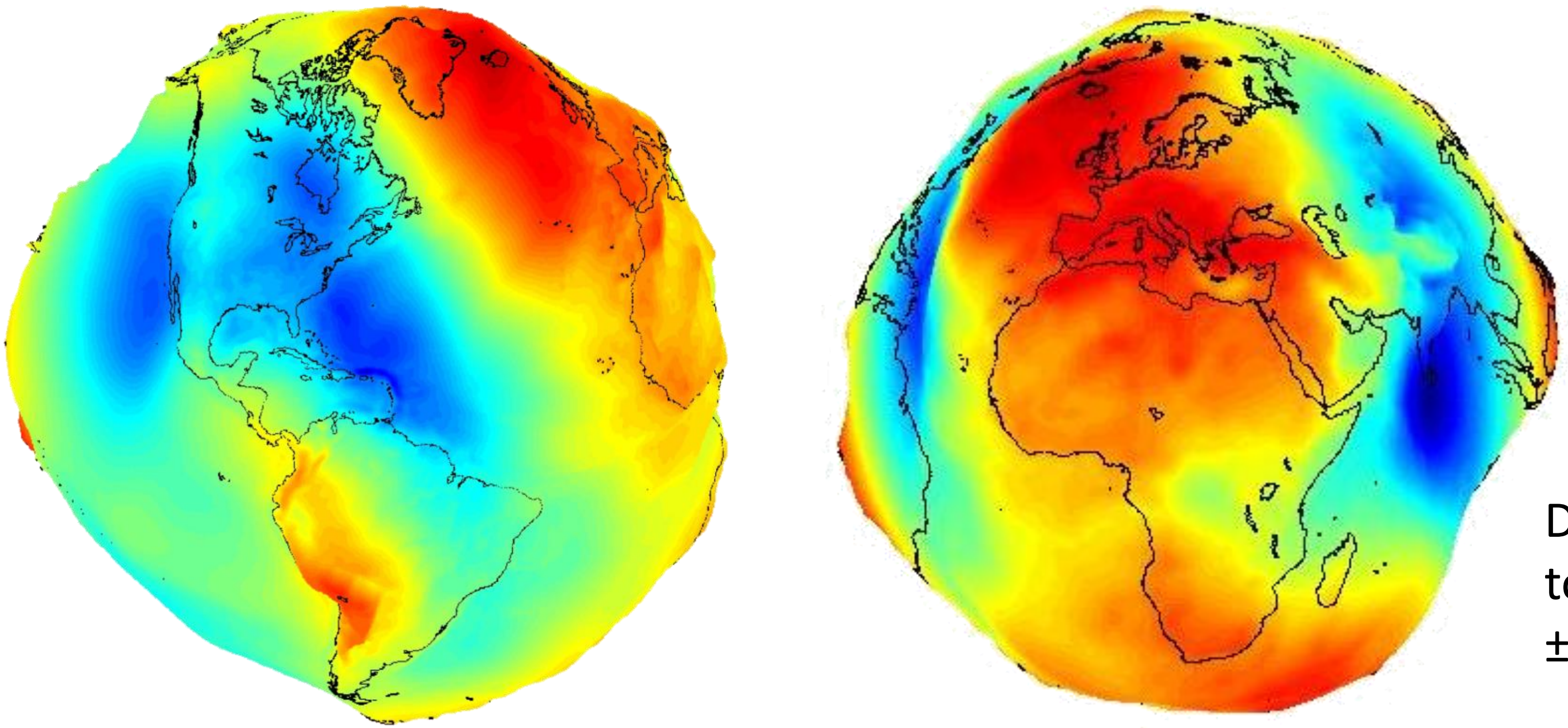

Departure to ellipticity: ± 100 m

Geoid: surface of constant gravitational + centrifugal potential energy, that coincides with the sea level at rest (no tides nor currents), continued below the continents.

(*The surface of a rotating fluid at equilibrium is an equipotential*)

In the absence of other forces: a ball placed on the geoid will not move

→ The **horizontal surface of reference**, over land and oceans = zero level of altitudes

Reference ellipsoid

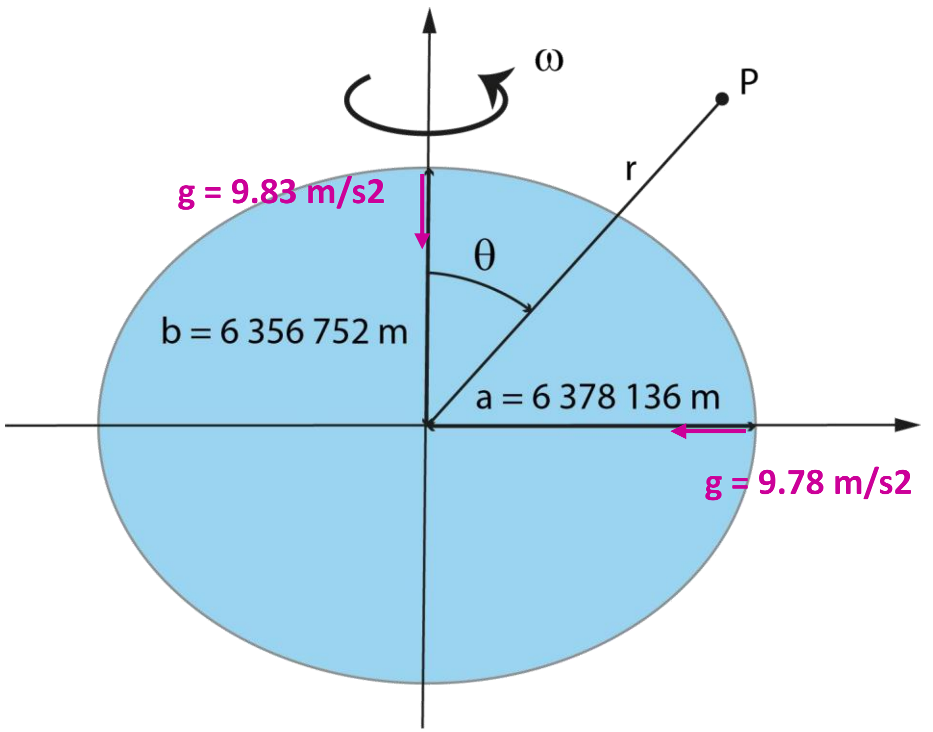

A dynamical definition:

Consider a homogeneous, rotating Earth with constant angular speed ϖ ;
total mass *M* includes the atmosphere.

Centrifugal potential: $V_{rot}(P) = \frac{1}{2}\,\varpi^2 r^2\ \sin\theta$

- Equipotential surfaces of its gravity potential U (gravitational + centrifugal) = ellipsoids

- Reference WGS84 ellipsoid:
  - centered on the barycenter of the Earth's masses
  - space geodesy $\rightarrow$ semi-major axis a, gravitational constant GM
  - global geoid model (C_{20}) $\rightarrow$ dynamical flattening

Thus this ellipsoid is based on the observed geoid flattening.

Non-hydrostatic geoid

- The observed flattening may be different from that of an Earth at hydrostatic equilibrium: it is indeed affected by the global-scale mantle density heterogeneity (Chambat et al., 2010).

- The non-hydrostatic geoid is defined with respect to hydrostatic state of reference: a radially-layered, rotating self-gravitating Earth.

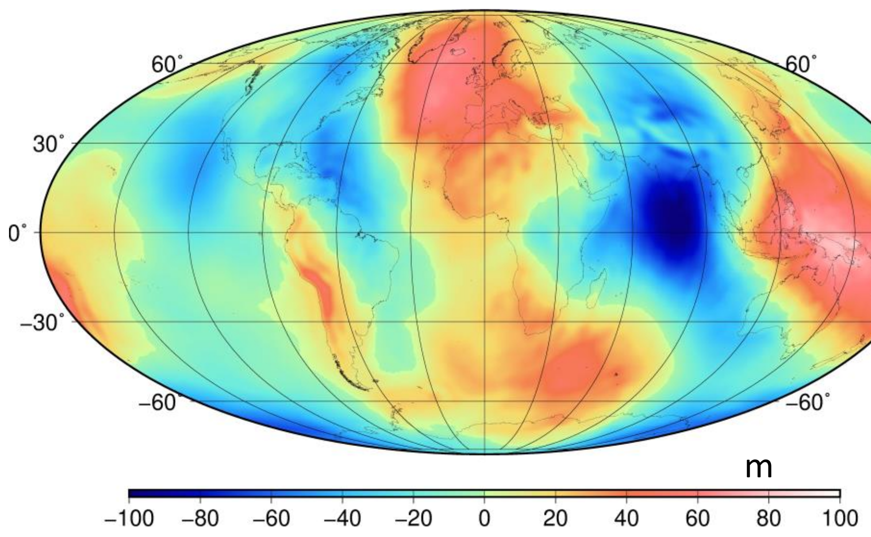

Geoid anomalies with respect to the WGS84 geodetic ellipsoid

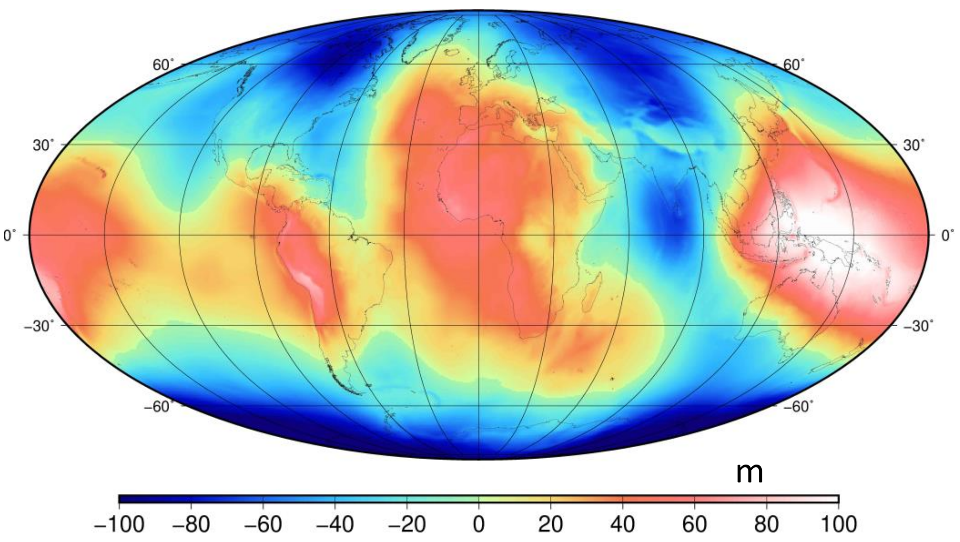

Geoid anomalies with respect to a hydrostatic, PREM-layered reference

Introduction to geodesy

1. A very old question: what is the shape of the Earth?

2. The revolution of the satellites

3. Gravity field from a static mass distribution and its spherical harmonics representation

4. Sources of the gravity field (geological timescales)

5. Time-varying gravity and surface displacements (timescales of weeks to secular)

Observing satellite motions

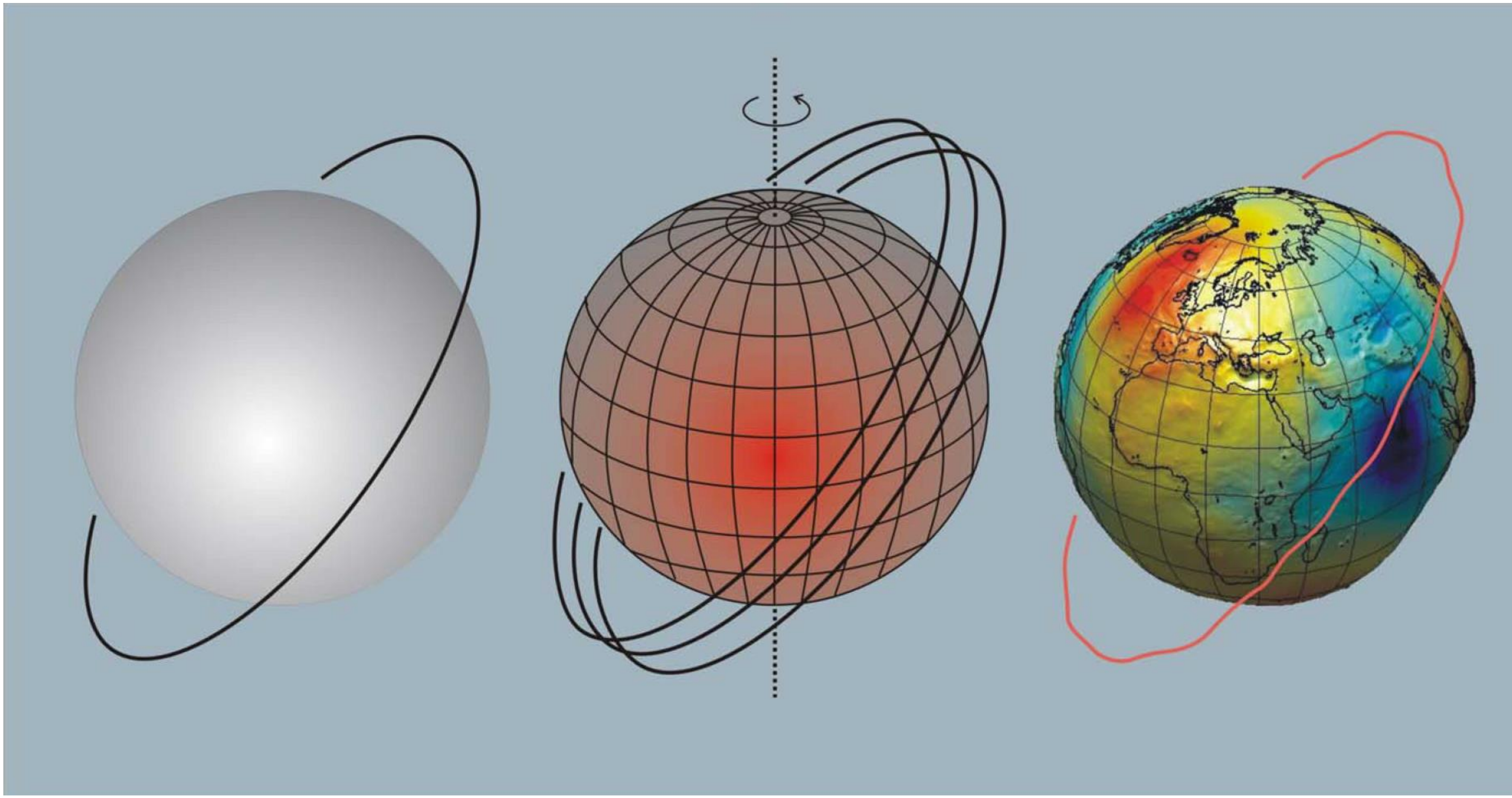

Source: Reiner Rummel

Homogeneous sphere $\rightarrow$ fixed elliptical orbit

Oblate spheroid $\rightarrow$ precessing elliptical orbit

(*Precession of orbital plane* $\rightarrow$ *dynamical flattening*)

Real Earth $\rightarrow$ orbit perturbations reflect the Earth's gravitational field

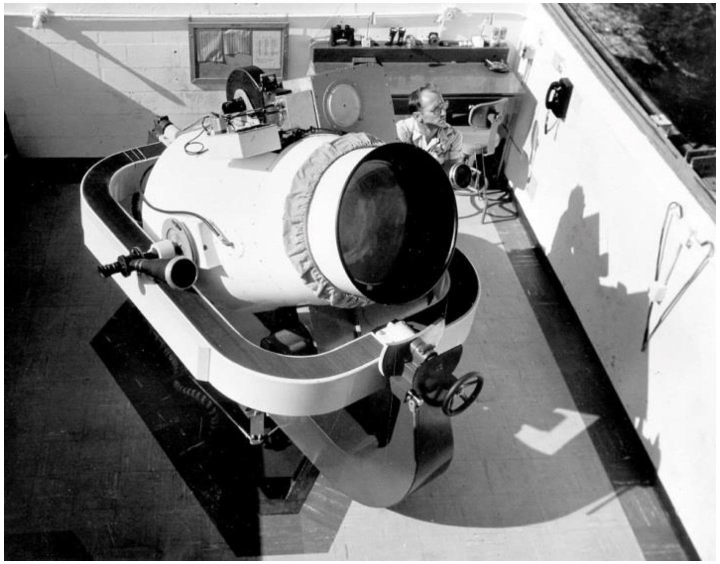

Baker-Nunn camera

A first global view of the geoid based on the tracking of satellites orbits using cameras

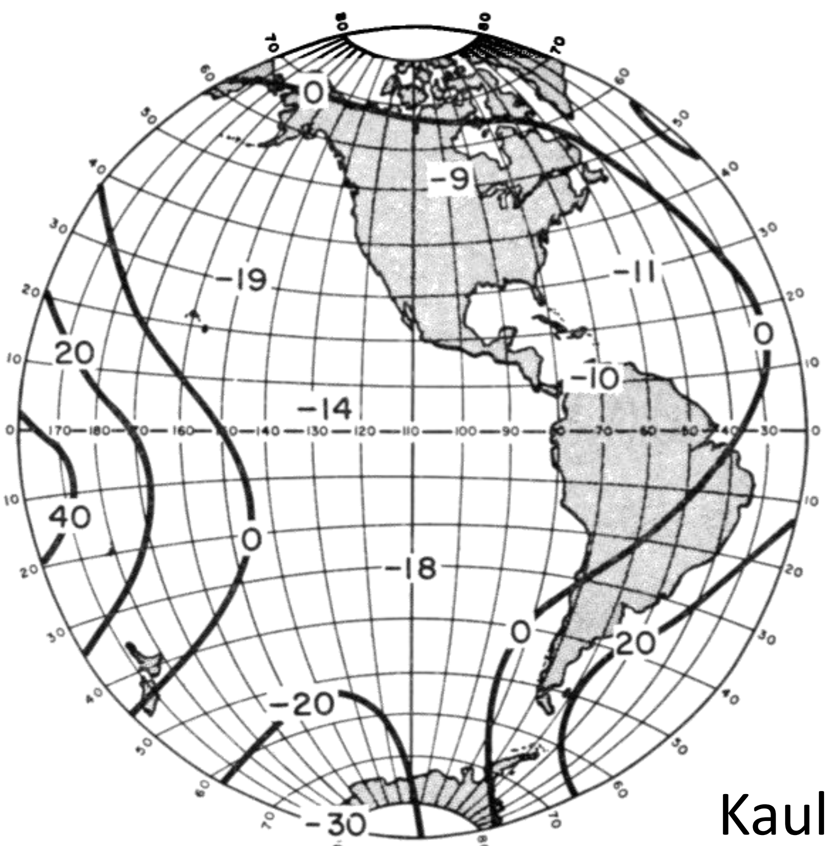

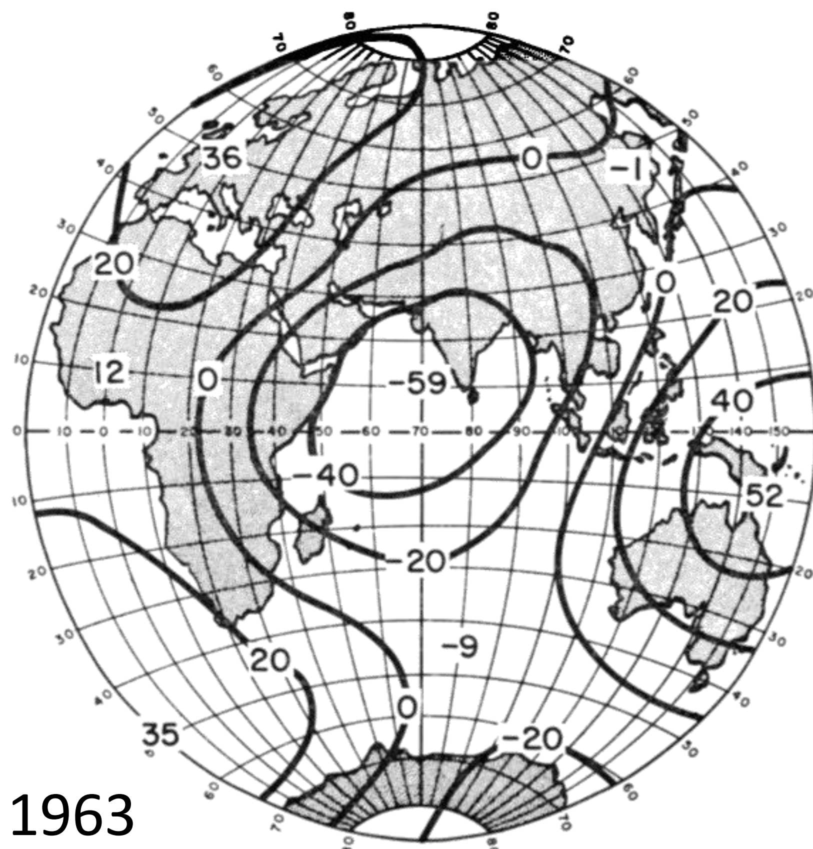

Kaula, 1963

Satellite laser ranging

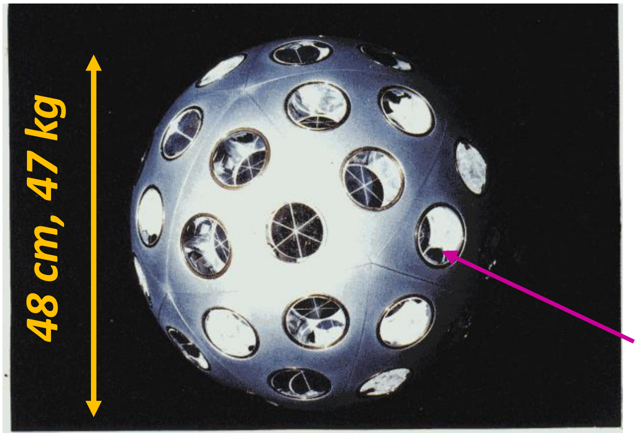

Retro-
reflectors

Starlette (CNES, launch 1975)

< 1 cm precision on the range measurement over 6000 km range

→ Earth's dynamical flattening (low degrees of the gravity field)

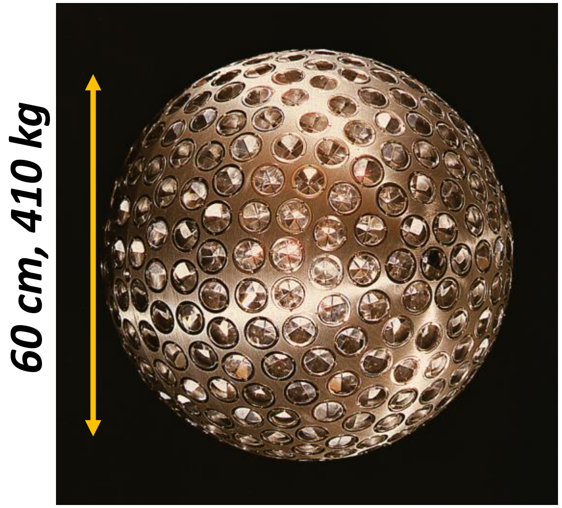

LAGEOS (launch 1976 & 1992)
5900 km altitude

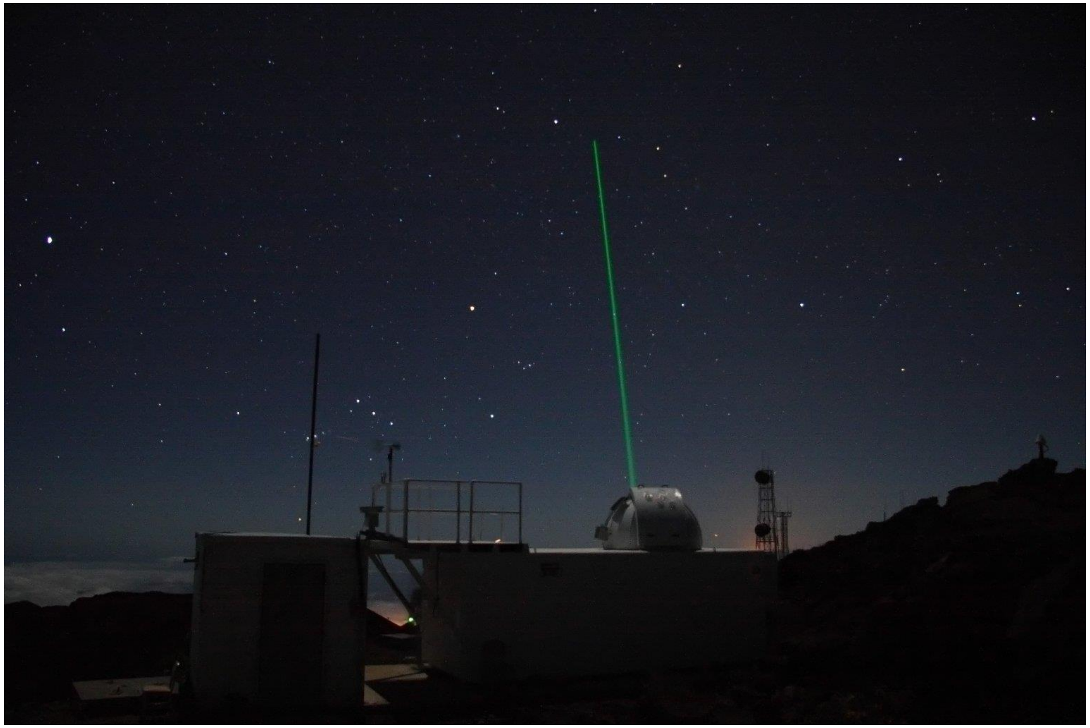

SLR station at Mt Haleakala, Maui island, Hawaii

The Earth gets less flat

Secular decrease: response to the last deglaciation

Inter-annual variations

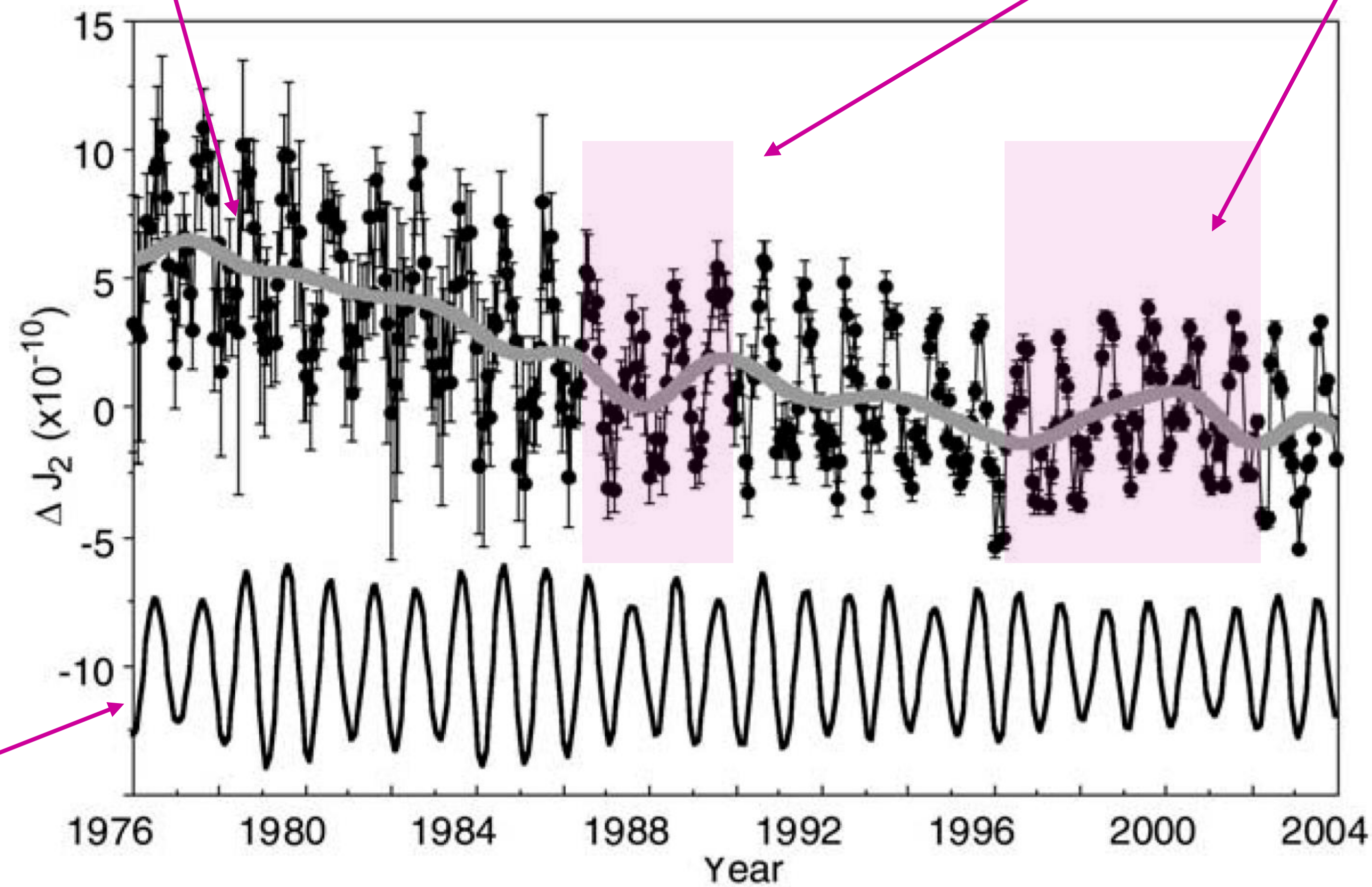

Seasonal variations

Cheng & Tapley (2004)

Variations of the Earth's dynamical flattening from satellite laser ranging

Tracking satellites from the ground

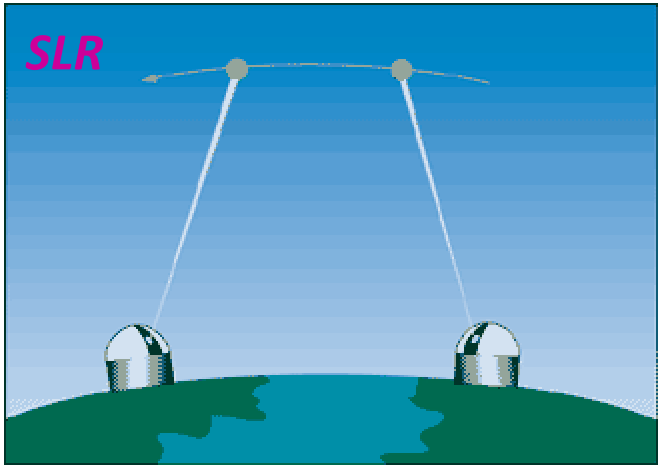

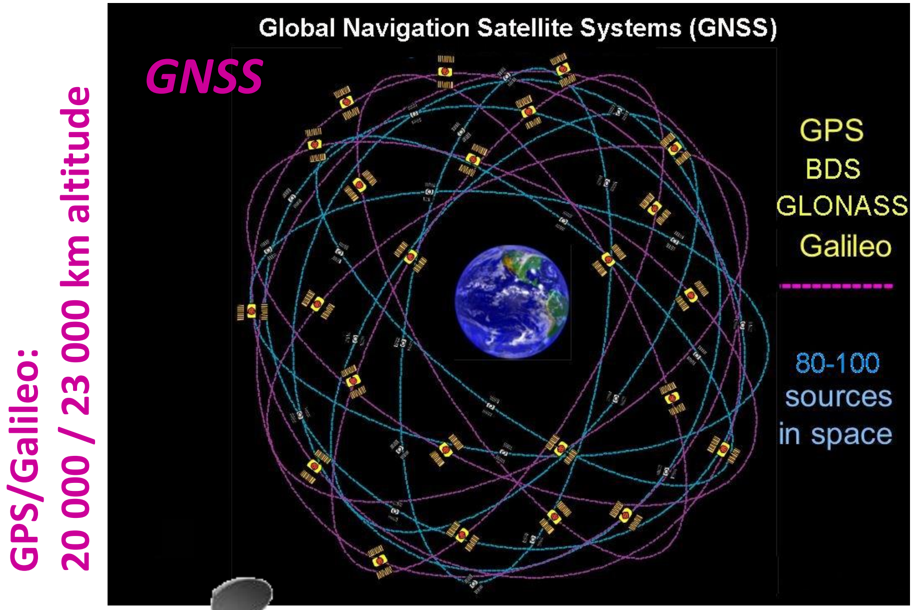

- Satellites have first been used to improve the gravity field and better model the orbits (ground stations positions known more accurately than the orbits).

- Improvements of the gravity field models → smaller orbit errors → study of the variations in the Earth's rotation.

- Good knowledge of the satellite position (its orbit) → improve ground station position → plate motions

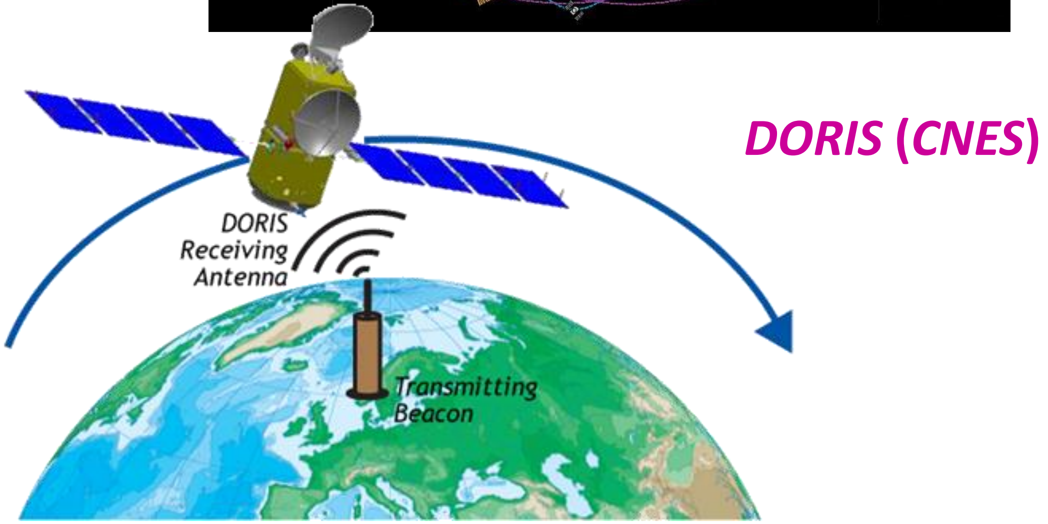

The GPS system: principle

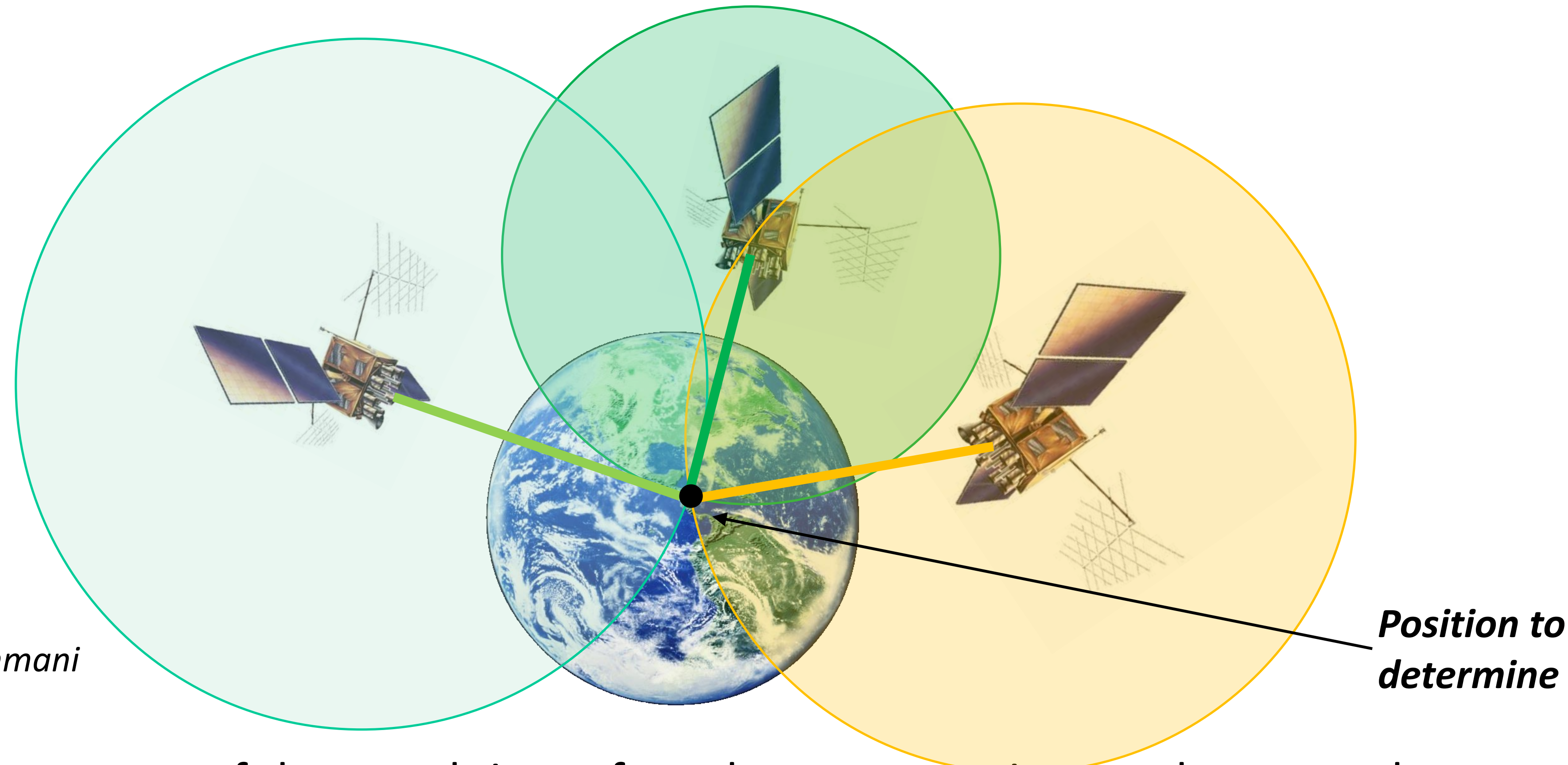

Image: Samuel Nahmani

- Measurement of the travel time of an electromagnetic wave between the satellite (emitter) and the ground station (receiver).
- If the position of 3 satellites is known, the 3 coordinates (x,y,z) of the ground station can be obtained.
- Non-linear equations $\rightarrow$ linearization $\rightarrow$ least-squares inversion of the ground station position.

Very Long Baseline Interferometry

• Delays between two arrivals at two antennas of microwave signals from an extra-galactic radio source (quasar) ; observe the delays associated with many different quasars.

- inertial frame defined by quasars
- relative positions of the antennas

$\rightarrow$ Earth's orientation in the inertial frame

Tsukuba, Japan

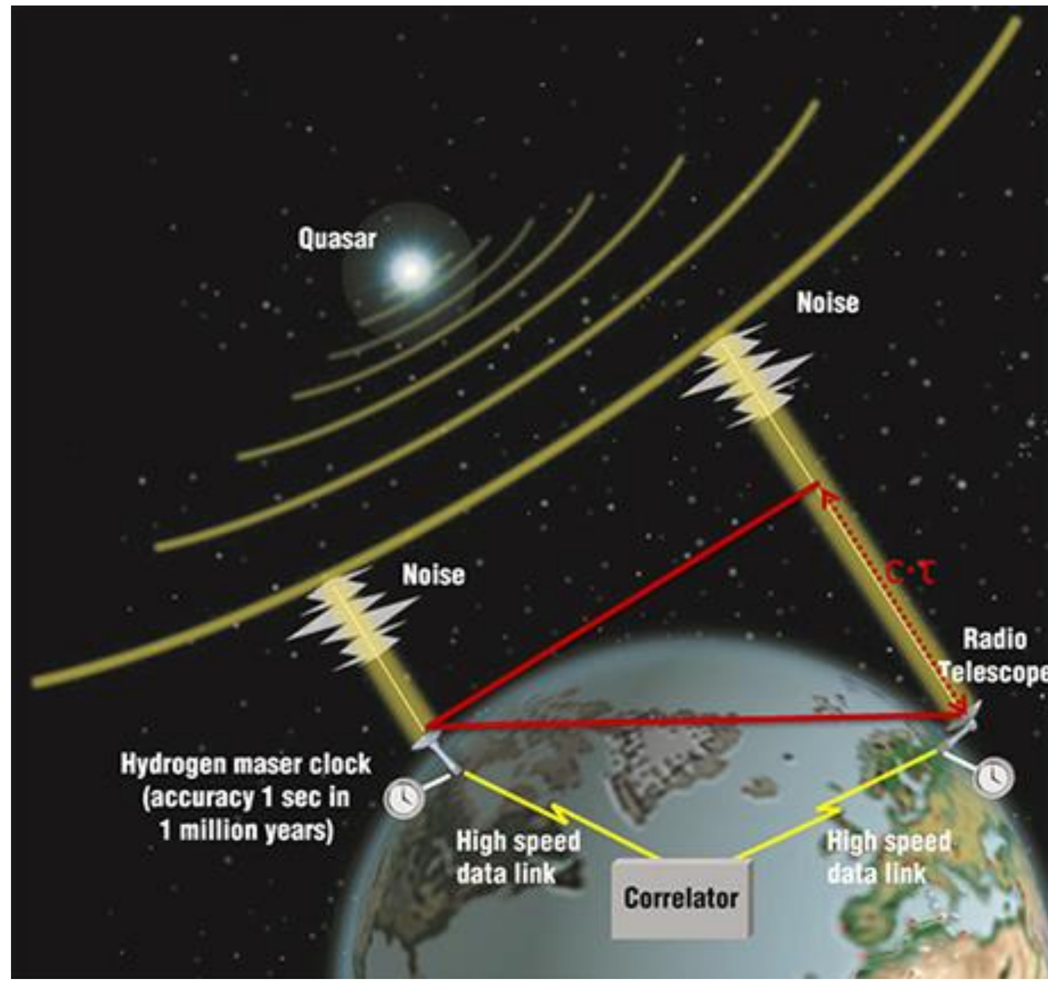

@ NASA

Network of space geodetic ground stations

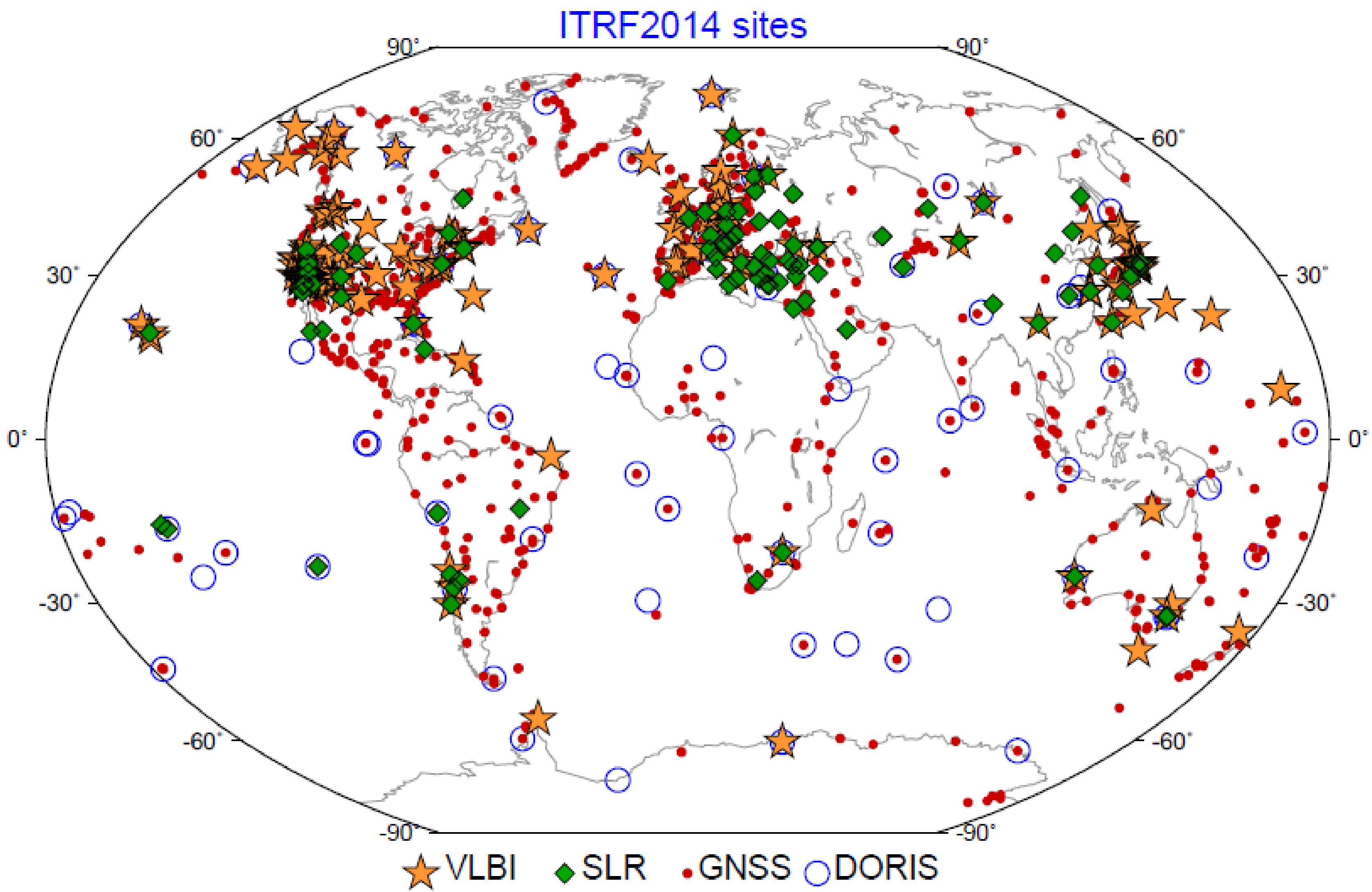

975 sites (1499 stations)

Altamimi et al. (2016)

Observing the plates kinematics

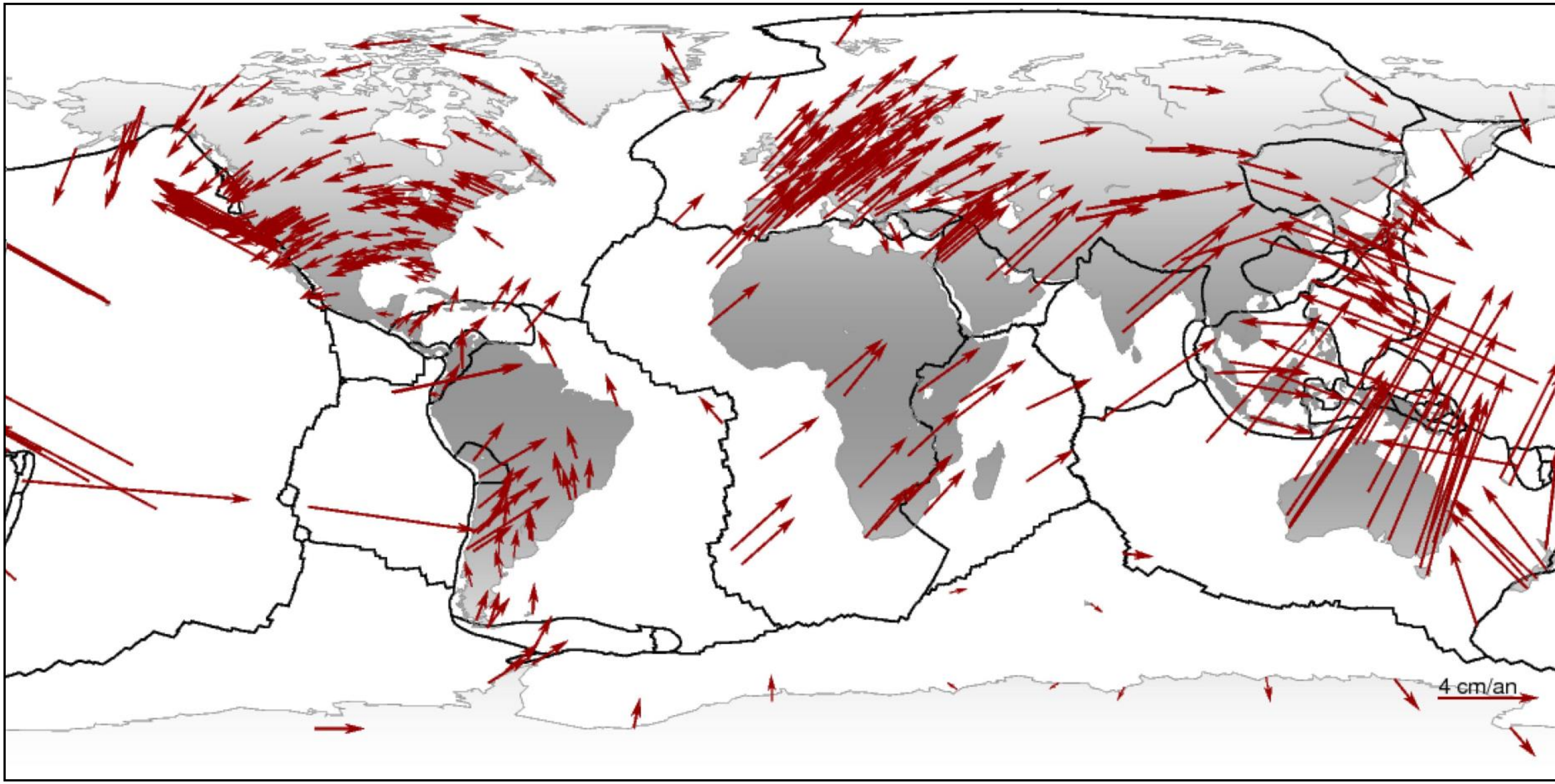

ITRF2008 horizontal velocities (Altamimi et al., 2014).

Good general agreement of the geodetic plate motion models with the geological ones over the last few millions of years.

A wealth of geodetic observations

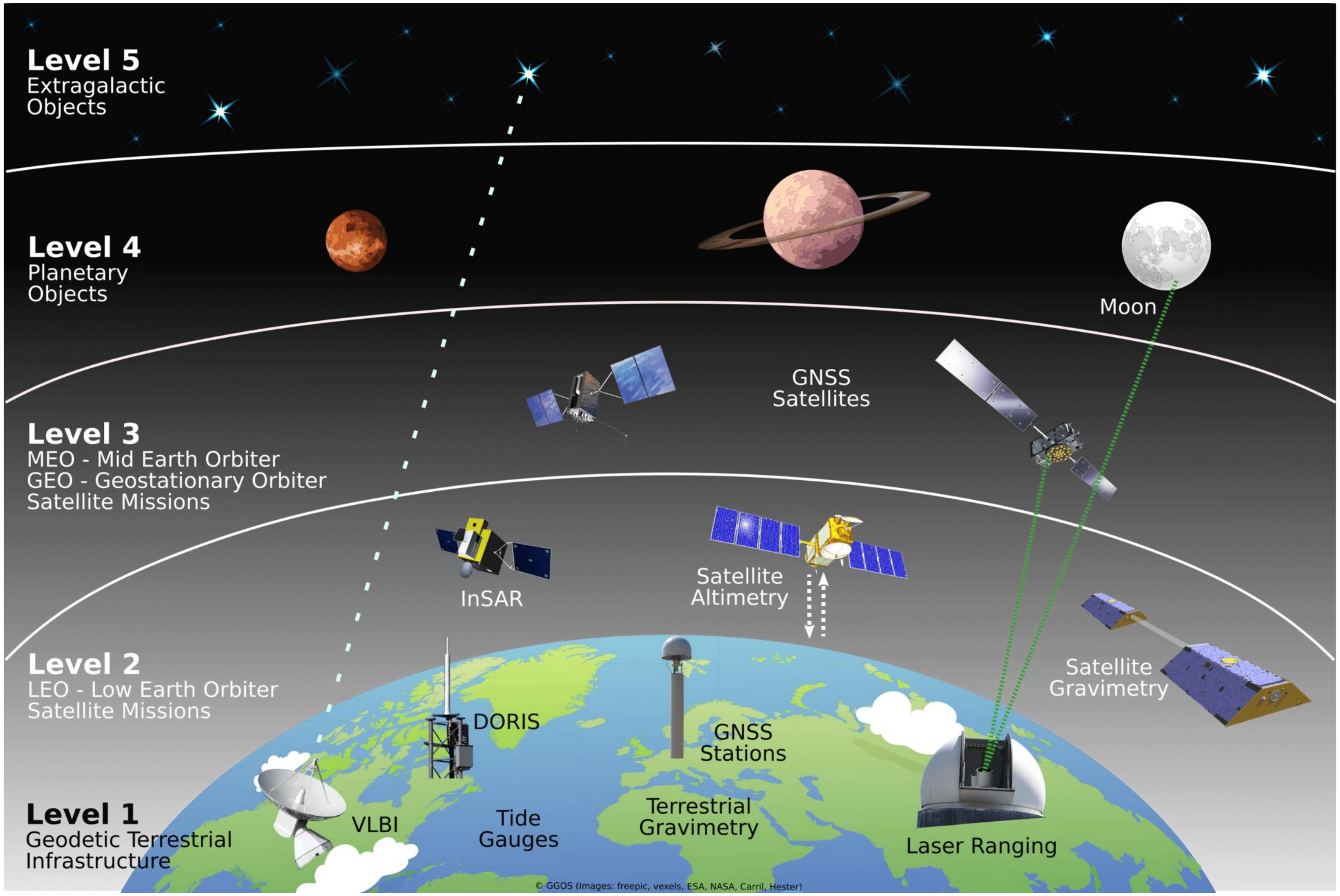

Accuracy on:

Positions: few mm

Velocities: 1 mm/yr, sometimes better

(both for the reference network of permanent stations)

Tracking the orbits not only from ground stations, but also from space (positioning using onboard GNSS receivers) $\rightarrow$ few cm accuracy on the orbits

Satellite altimetry and the marine gravity field

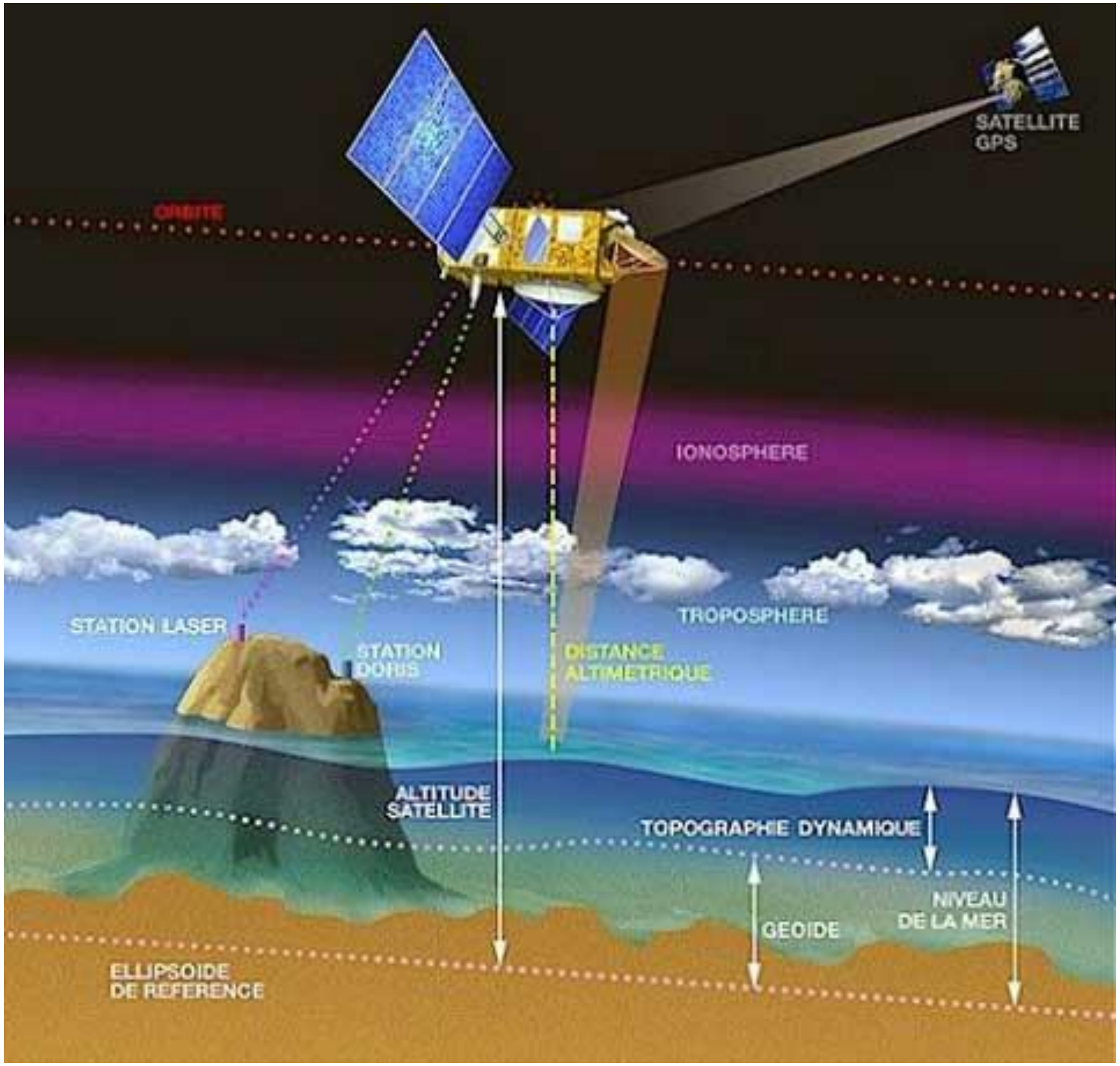

Distance between the satellite and the sea surface from the round-trip time of a radar pulse.

Satellite positioning: DORIS, GPS

Orbital height ~ 1300 km (Topex, Jason) ; 800 km (Saral)

Topex-Poseidon

Jason 1

Saral-AltiKa

A whole series of satellites since 1978

The marine gravity field

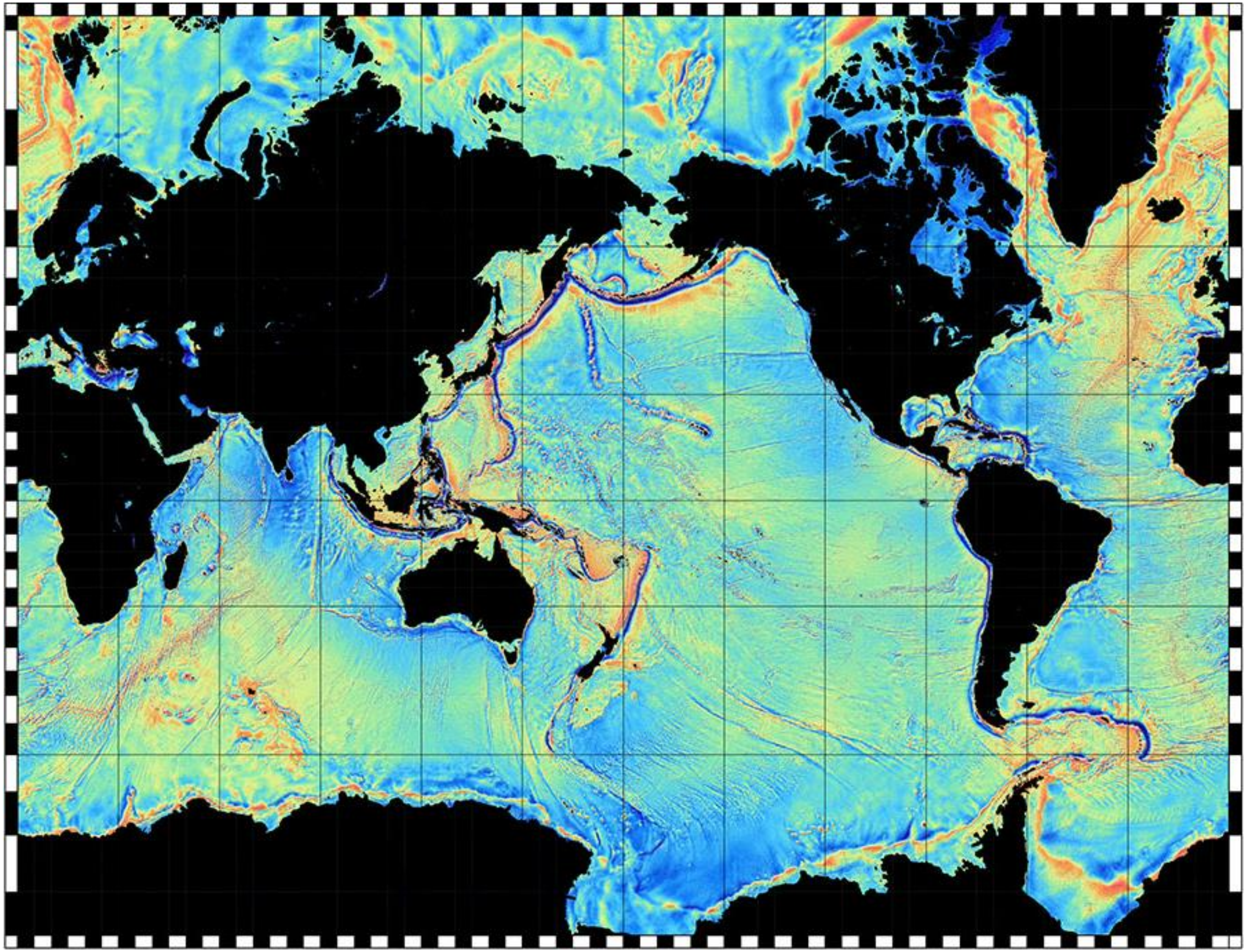

Smith & Sandwell (1997)
Andersen & Knudsen (1998)

Anomalies of intensity of gravity
(reference ellipsoid contribution removed)

Mapping of uncharted seamounts

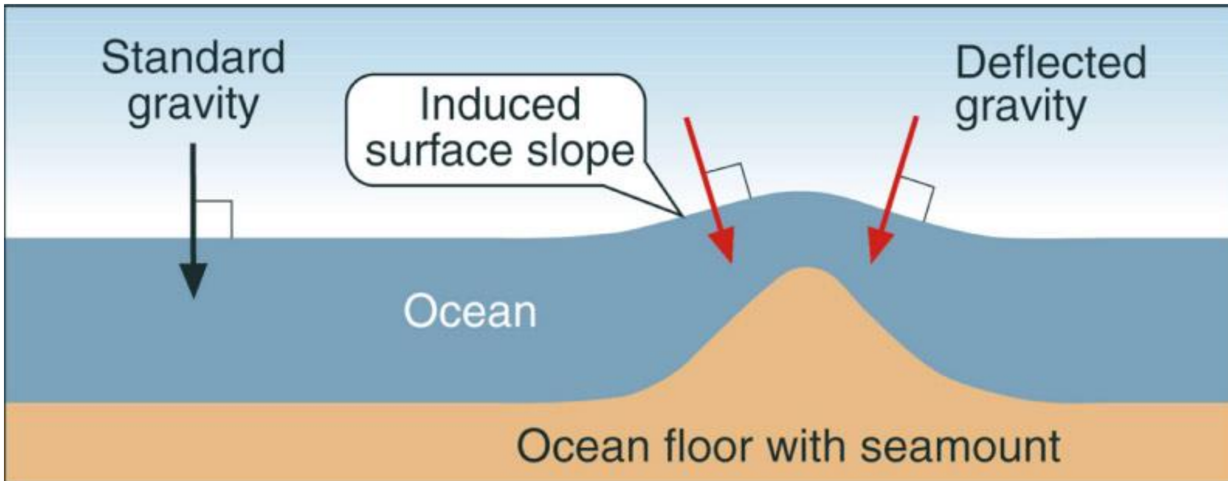

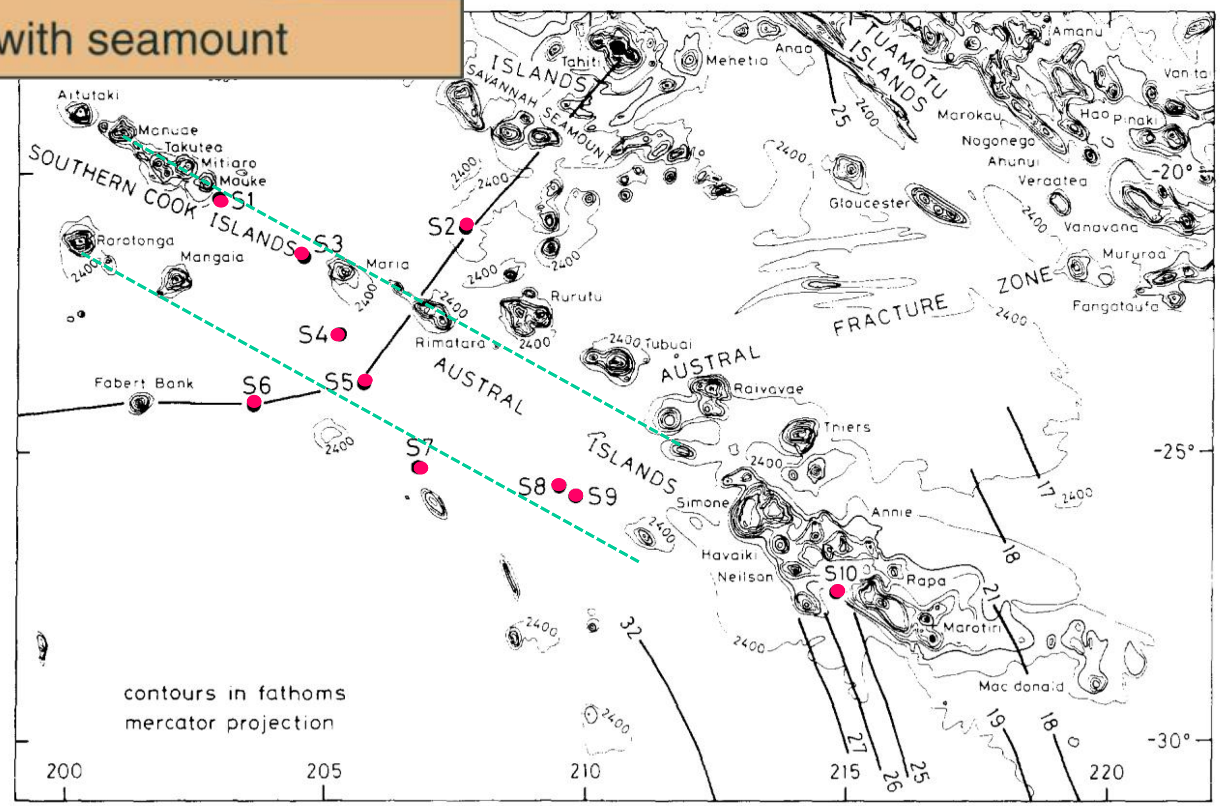

Cook-Austral volcanic chain, South Central Pacific

Evidence for 2 parallel lines of volcanoes

Diament & Baudry (1987)

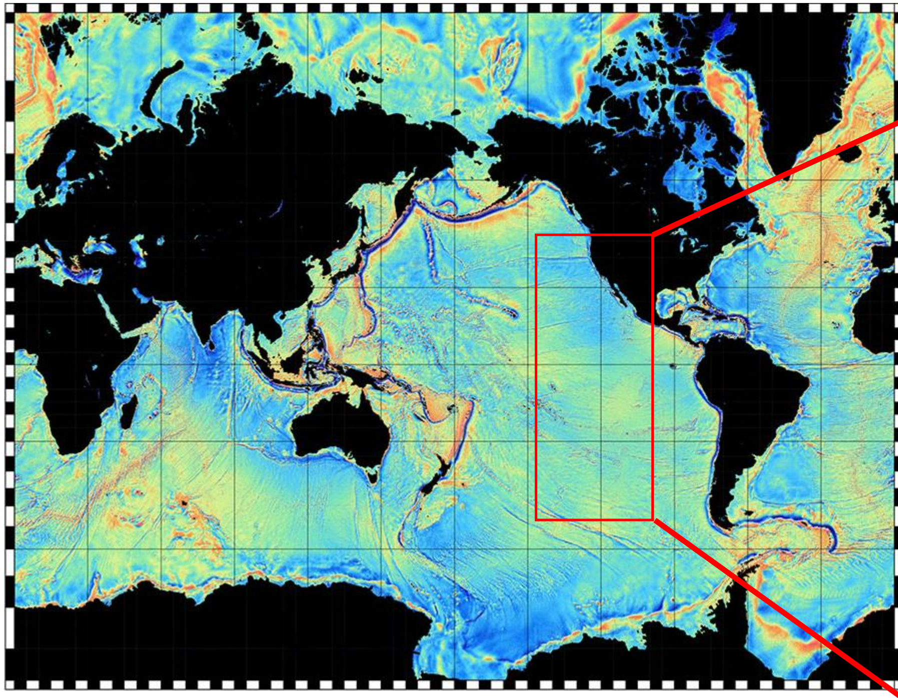

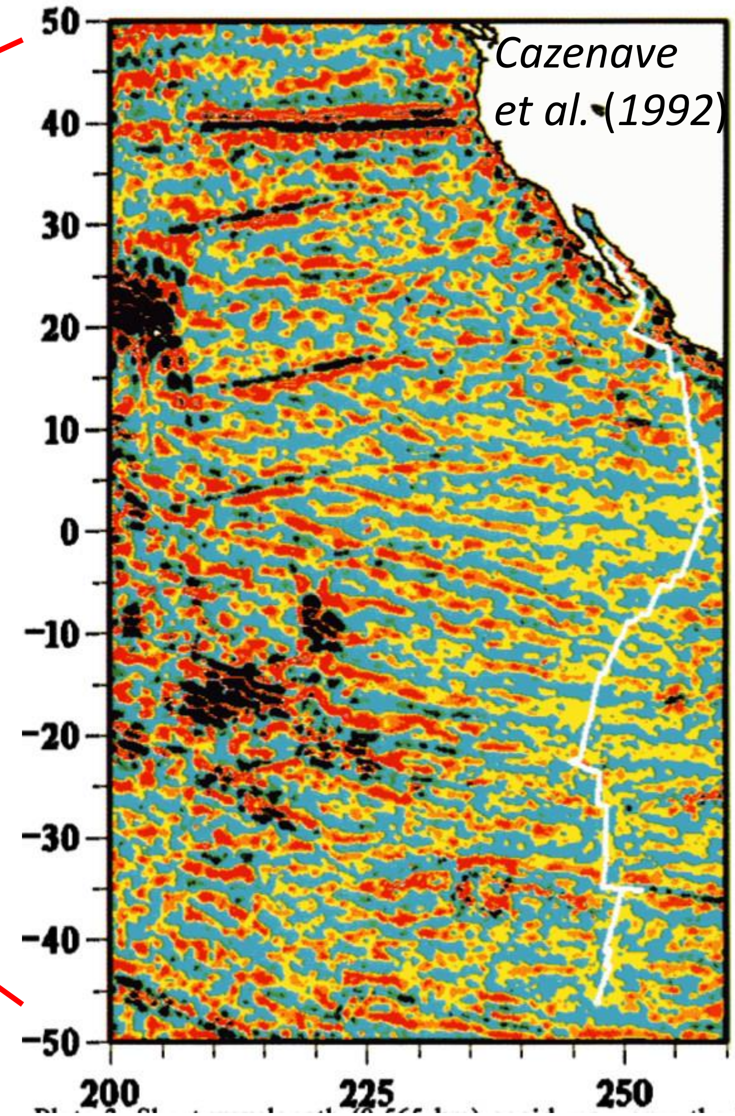

‘small’ (200-300 km) scale geoid undulations parallel to plate motion

Different mechanisms proposed.

Volcanism above the upwellings → secondary convection driven by plate motion (Buck & Parmentier, 1986 ; Robinson & Parsons 1988)

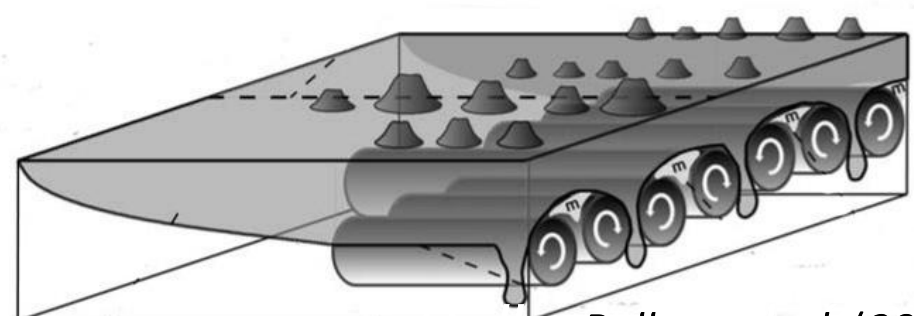

Ballmer et al. (2007)

Satellite gravity missions

CHAMP g

GRACE $g(t)$

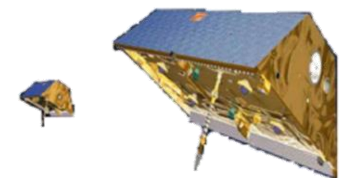

GOCE $\vec{g}$

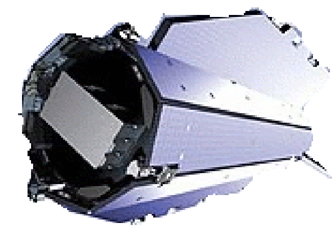

High-resolution mapping of the Earth's gravity:

- – Fly low (higher sensitivity to smaller scale structures)
- – Carry out dedicated gravity observation systems
- – Measure the satellite position continuously (GNSS, SLR)
- – Measure / compensate non-gravitational forces (accelerometry)

Introduction to geodesy

1. A very old question: what is the shape of the Earth?

2. The revolution of the satellites

3. Gravity field from a static mass distribution and its spherical harmonics representation

4. Sources of the gravity field (geological timescales)

5. Time-varying gravity and surface displacements (timescales of weeks to secular)

Gravitational field of a mass source

- A mass M in $\boldsymbol{x_0}(x_0,y_0,z_0)$ generates a gravitational field or acceleration $\boldsymbol{g}$ in the whole space:

At $\boldsymbol{x}(x,y,z)$: $$\boldsymbol{g}(x,y,z) = \frac{GM(\boldsymbol{x}-\boldsymbol{x}_0)}{|\boldsymbol{x}-\boldsymbol{x}_0|^3}$$

G = 6.67 10^{-11} SI ($m^3.kg^{-1}.s^{-2}$)

- The field $\boldsymbol{g}$ derives from a scalar potential V:

$$\boldsymbol{g} = -\boldsymbol{\nabla} V$$

V = potential energy per unit mass

Equipotential surfaces (orthogonal to ***g****)*

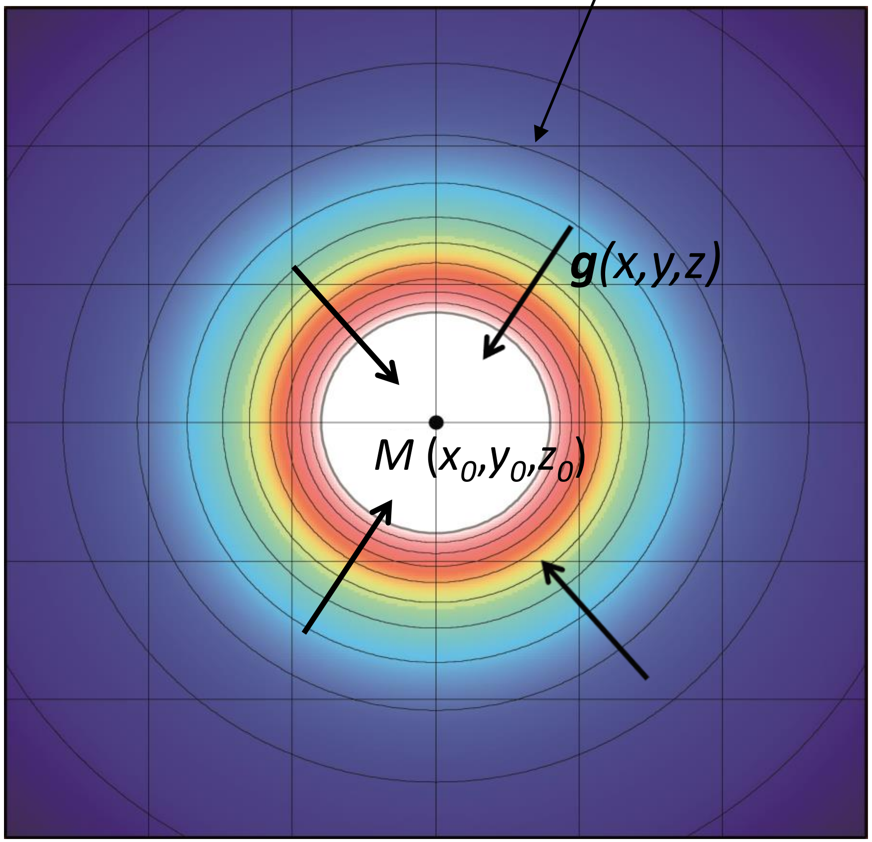

- A mass m at point $\boldsymbol{x}(x,y,z)$ feels the gravitational force $\boldsymbol{F} = m\,\boldsymbol{g}(x,y,z)$
  = mutual attraction between two masses

Newton's law of gravity

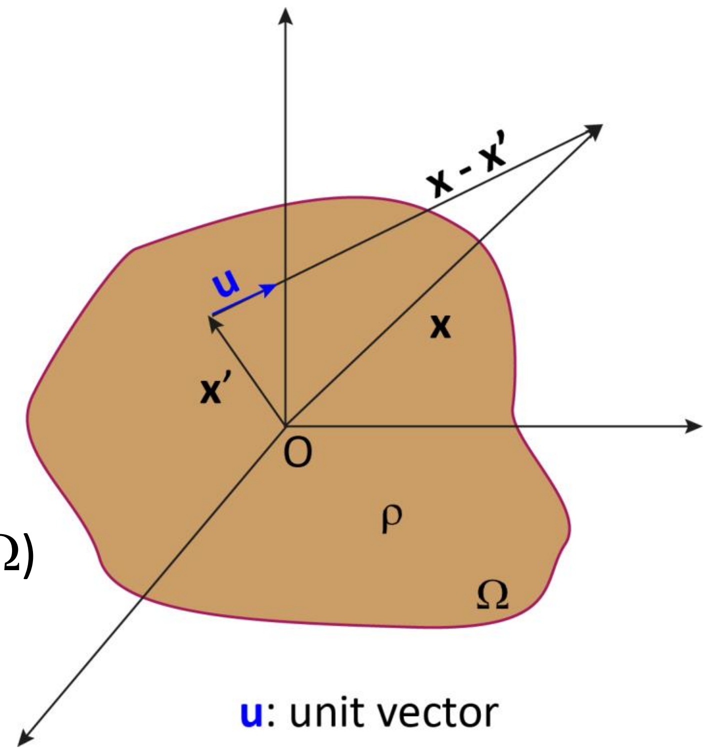

u: unit vector

$$\boldsymbol{u} = \frac{(\boldsymbol{x} - \boldsymbol{x}')}{|\boldsymbol{x} - \boldsymbol{x}'|}$$

- For a mass density $\rho(x',y',z')$ in a volume Ω:

At $\boldsymbol{x}(x,y,z)$: $\boldsymbol{g}(x,y,z) = \int_\Omega \frac{G\rho(\boldsymbol{x}')(\boldsymbol{x}-\boldsymbol{x}')}{|\boldsymbol{x}-\boldsymbol{x}'|^3} d^3\boldsymbol{x}'$

(Replace M by the mass element $\rho(\boldsymbol{x}')d^3\boldsymbol{x}'$ and sum over Ω)

And: $\boxed{V(x,y,z) = \int_\Omega \frac{G\rho(\boldsymbol{x}')}{|\boldsymbol{x}-\boldsymbol{x}'|} d^3\boldsymbol{x}'}$ (1)

- Another formulation of this law is the **Poisson equation**:

Consider the Laplacian operator: $\Delta V = \partial_x^2 V + \partial_y^2 V + \partial_z^2 V$

Replace in equation (1), we end up with: $\boxed{\Delta V(x,y,z) = -4\pi G\rho(x,y,z)}$

A harmonic potential

- Outside the mass sources, the Poisson equation becomes the **Laplace equation**:

$$\boxed{\Delta V(x, y, z) = 0}$$

- Thus, *V* is harmonic outside the masses

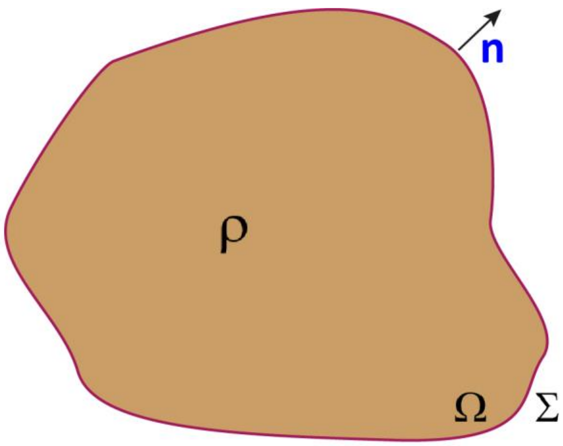

n: unit vector, normal to the surface Σ

<u>A strong property</u>:

Suppose V or $\partial_n V$ is known on the surface Σ bounding the volume Ω of the sources. Then *V* is entirely and uniquely determined in the whole space outside Σ.

Spherical harmonics representation

Newton integral: $V(x,y,z) = \int_\Omega \frac{G\rho(\boldsymbol{x'})}{|\boldsymbol{x}-\boldsymbol{x'}|} d^3\boldsymbol{x'}$

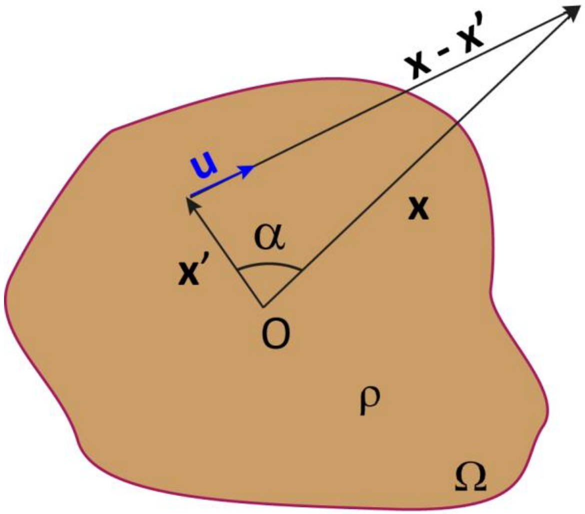

1. Development of $\frac{1}{|\boldsymbol{x}-\boldsymbol{x'}|}$:

$$\frac{1}{|\boldsymbol{x}-\boldsymbol{x}'|} = \frac{1}{|\boldsymbol{x}|}\sum_{\ell=0}^{\infty}\left(\frac{|\boldsymbol{x}'|}{|\boldsymbol{x}|}\right)^{\ell} P_\ell(\cos\alpha)$$

Legendre polynomial of degree l

2. Addition theorem:

$$(2\ell+1)P_\ell(\cos\alpha) = \sum_{m=-\ell}^{\ell} Y_\ell^{m,*}(\theta,\varphi)\, Y_\ell^{m}(\theta',\varphi')$$

Surface spherical harmonics of degree l and order m

Spherical coordinates: $\boldsymbol{x}(r,\theta,\varphi)$

$\boldsymbol{x'}(r',\theta',\varphi')$

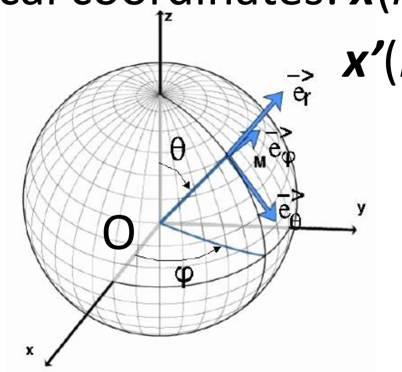

Frame centered at point O

$\rightarrow$ insert 1 and 2 in Newton integral

Spherical harmonics representation

We end-up with:

Attenuation with altitude !!

$$V(r,\theta,\varphi) = \frac{GM}{a}\sum_{\ell=0}^{\infty}\sum_{m=-\ell}^{\ell}\left(\frac{a}{r}\right)^{\ell+1} v_{\ell,m}\, Y_\ell^m(\theta,\varphi)$$

Semi-major axis

The coefficients of this development are a weighted integral of the densities inside the Earth:

$$v_{\ell,m} = \frac{1}{2\ell+1}\,\frac{1}{M\,a^\ell}\int_\Omega r'^{\ell}\,\rho(r',\theta',\varphi')\,Y_\ell^m(\theta',\varphi')\,d\Omega(r',\theta',\varphi')$$

The Y_ℓ^m are the fully normalized spherical harmonics:

$$Y_\ell^m(\theta,\varphi) = N_{\ell,m}\,P_{\ell,m}(\cos\theta)\,\cos m\varphi \qquad m \geq 0$$
$$Y_\ell^m(\theta,\varphi) = N_{\ell,|m|}\,P_{\ell,|m|}(\cos\theta)\,\sin|m\varphi| \qquad m < 0$$

The normalization factor $N_{\ell,m}$ is such that: $\frac{1}{4\pi}\iint_{unit\ sphere}|Y_\ell^m(\theta,\varphi)|^2\sin\theta\, d\theta\, d\varphi = 1$

Spherical harmonics representation

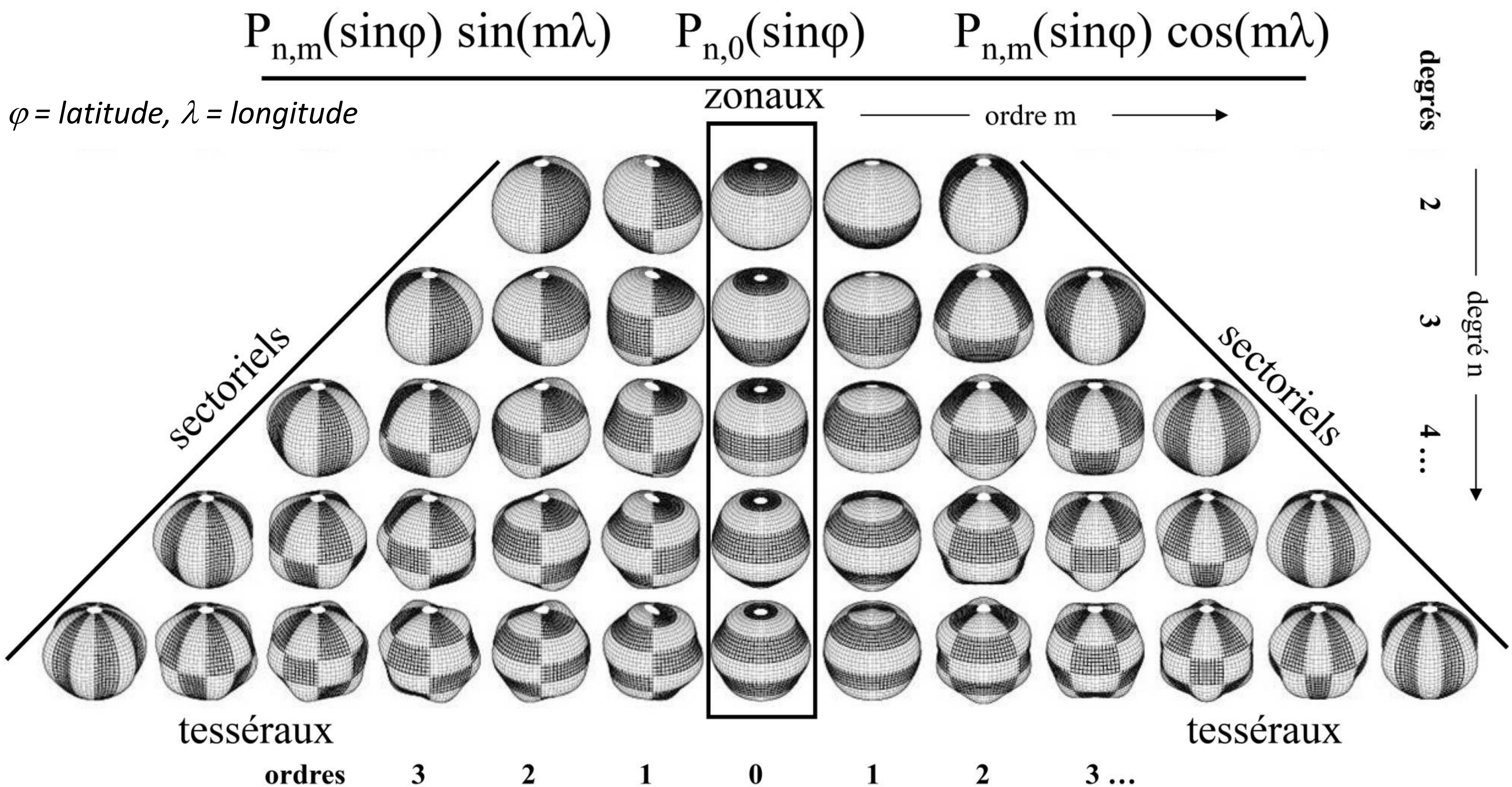

φ = latitude, λ = longitude

Spatial wavelength for each degree: $\frac{\lambda}{2} = \frac{20\,000\ km}{\ell}$

Source: Richard Biancale

The low degree coefficients

We usually note $C_{\ell,m}$ the coefficients of the cosine harmonics ($m \geq 0$) and $S_{\ell,m}$ those of the sine harmonics ($m < 0$).

- Degree 1:

$$C_{1,0} = \frac{z_G}{a} \;\; ; \;\; C_{1,1} = \frac{x_G}{a} \; ; \; S_{1,1} = \frac{y_G}{a}$$

- Degree 2:

$$C_{2,0} = -\frac{1}{Ma^2}\left(C - \frac{A+B}{2}\right)$$

squared distance to z rotation axis

C: principal moment of inertia (polar) : $C = \int_\Omega \left(x'^2 + y'^2\right)\rho(r',\theta',\varphi')d\Omega(r',\theta',\varphi')$

A, B : principal moments of inertia (equatorial):

$$\mathrm{A} = \int_\Omega \left(y'^2 + z'^2\right)dm(r',\theta',\varphi') \;\; ; B = \int_\Omega \left(x'^2 + z'^2\right)dm(r',\theta',\varphi')$$

Gravity field models

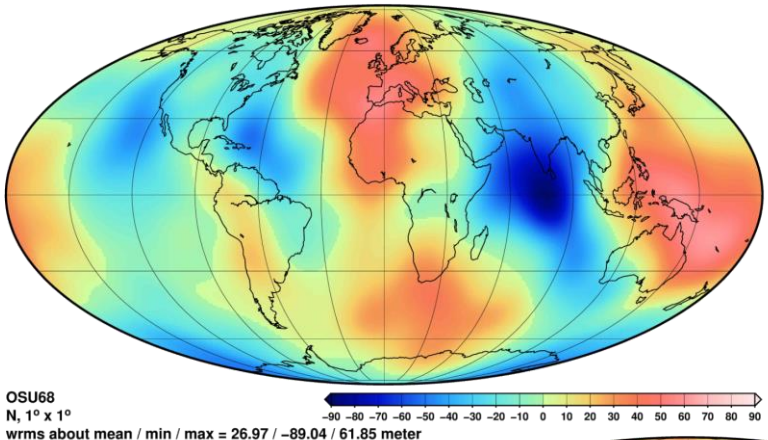

1968
Ground gravity
Satellites

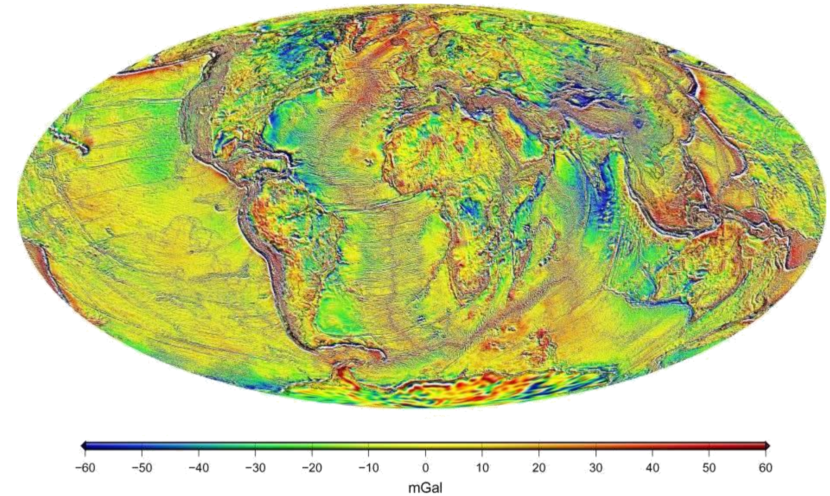

2008 - Including GRACE (static)

1975
Satellites only

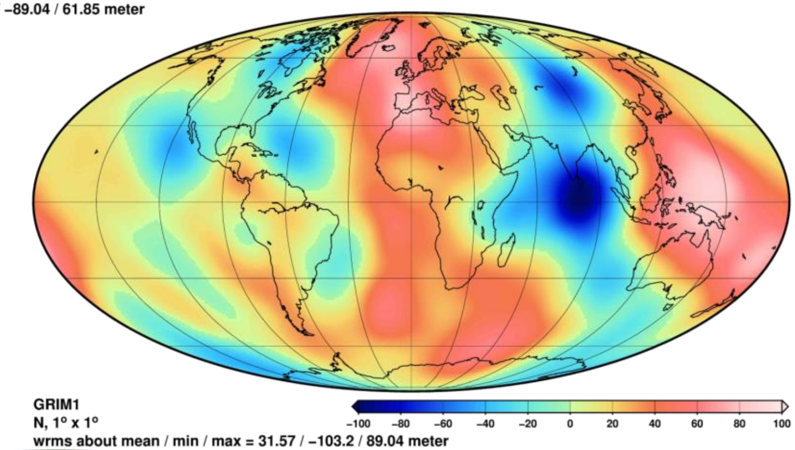

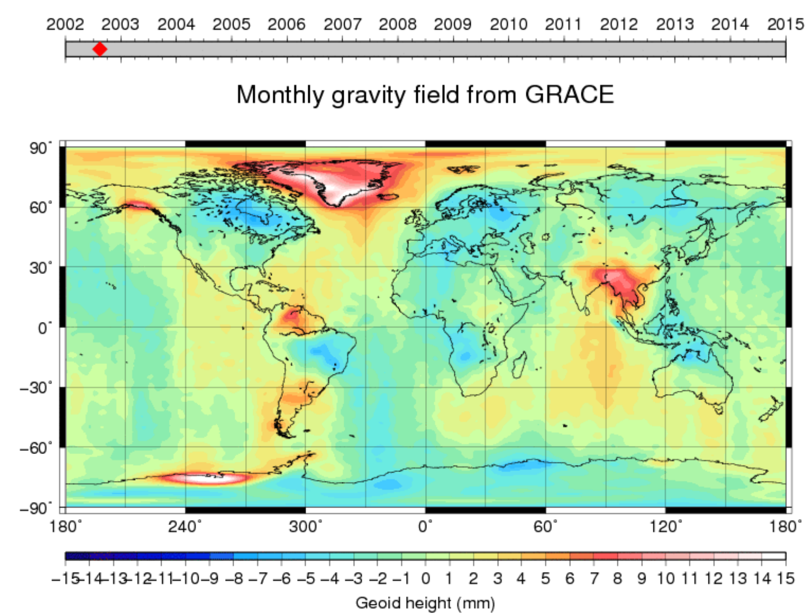

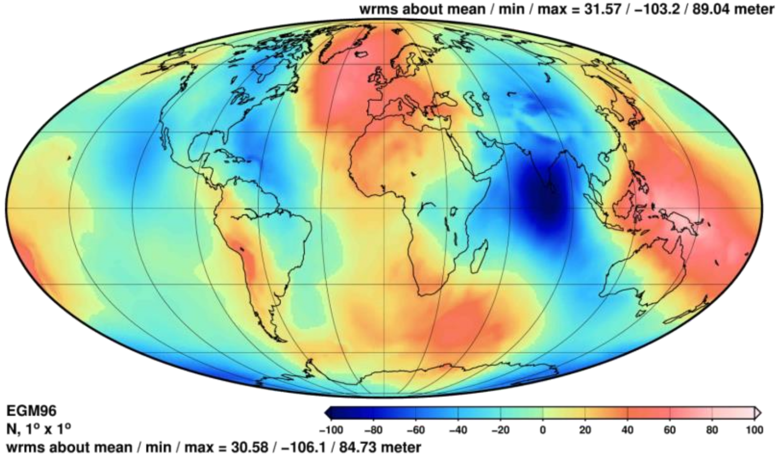

1996
Ground gravity
Satellites
Altimetry

2015 – Time-varying gravity

Introduction to geodesy

1. A very old question: what is the shape of the Earth?

2. The revolution of the satellites

3. Gravity field from a static mass distribution and its spherical harmonics representation

4. Sources of the gravity field (geological timescales)

5. Time-varying gravity and surface displacements (timescales of weeks to secular)

Removal of the topographic contribution

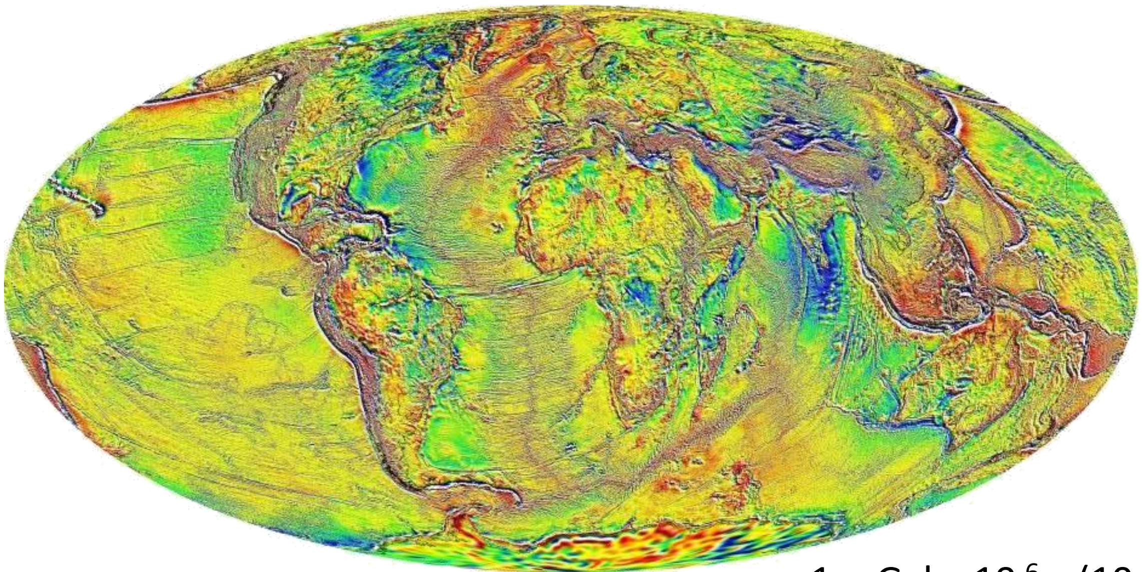

World gravity map
Bureau Gravimétrique International

1 mGal = 10^{-6} x (10 m/s^2)

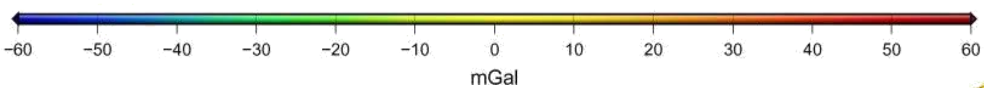

Free-air gravity anomalies
(reference ellipsoid removed)

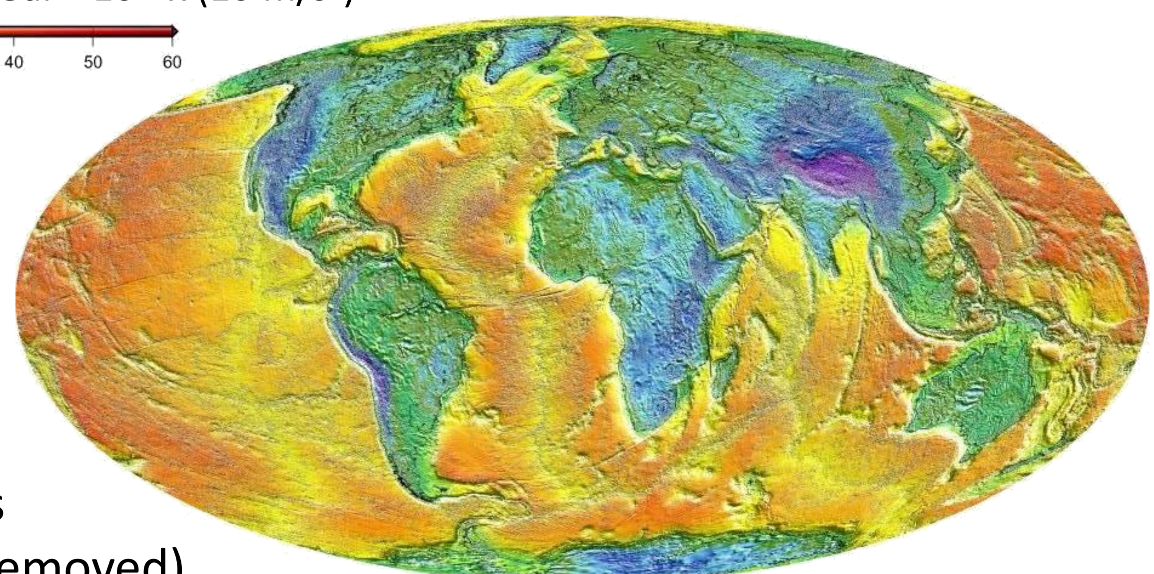

Bouguer gravity anomalies
(surface topography also removed)

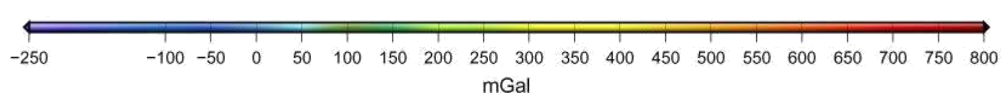

Isostatic support of the topographies

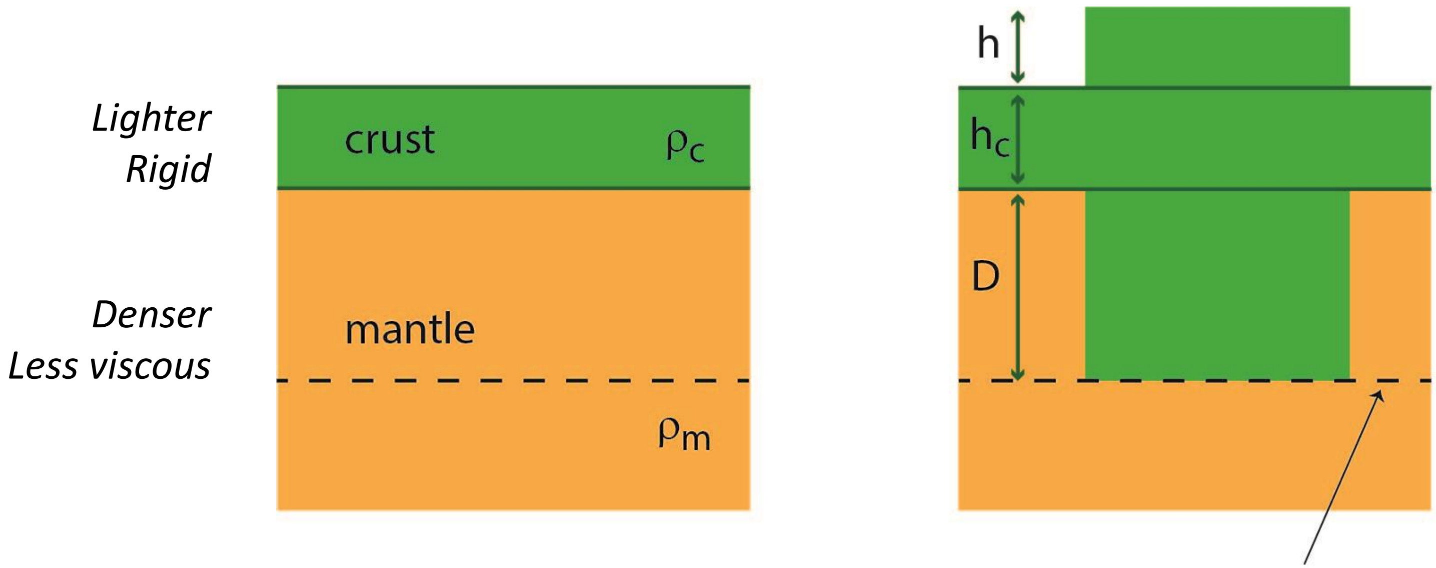

Archimedes principle:

The excess topographic weight is buoyed by the default weight of the crustal root.

hydrostatic compensation surface:

$$P = \rho_c \, g \, h_c + \rho_m \, g \, D = \rho_c \, g \, (h + h_c + D) = cstt$$

Airy model (1855): $D = \dfrac{\rho_c}{\rho_m - \rho_c} h \quad \rightarrow \quad D = 5.4\, h\,;$ $\qquad \rho_c = 2700 kg.m^{-3}$, $\rho_m - \rho_c = 500 kg.m^{-3}$

A weak crust responding locally and intensely to a load

Isostatic support of the topographies

Everest (*1790-1866*)

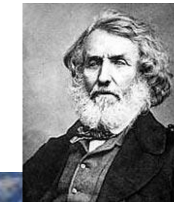

Pratt model (1854)

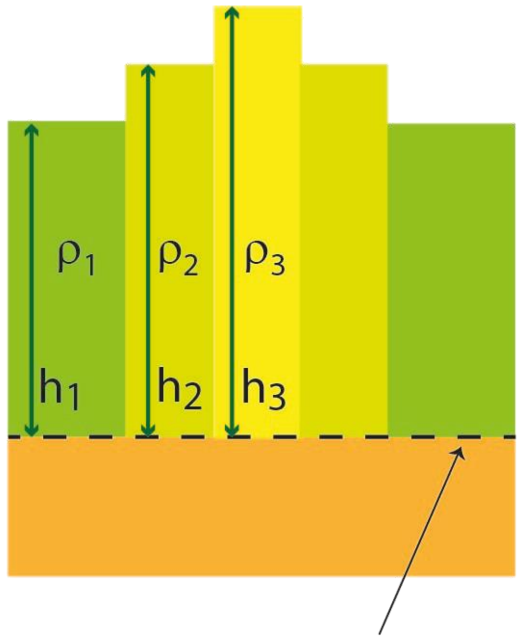

hydrostatic compensation surface:

$$P = \rho_1 \, g \, h_1 = \rho_2 \, g \, h_2 = \rho_3 \, g \, h_3 = cstt$$

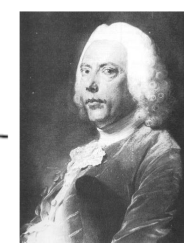

Bouguer (*1698-1758*)

- Moutains roots, surface load: Airy model
- Topographies associated with thermal variations due to a heat source: Pratt model

Example: crustal thickness

Both Pratt and Airy models have been used to estimate the crustal thickness

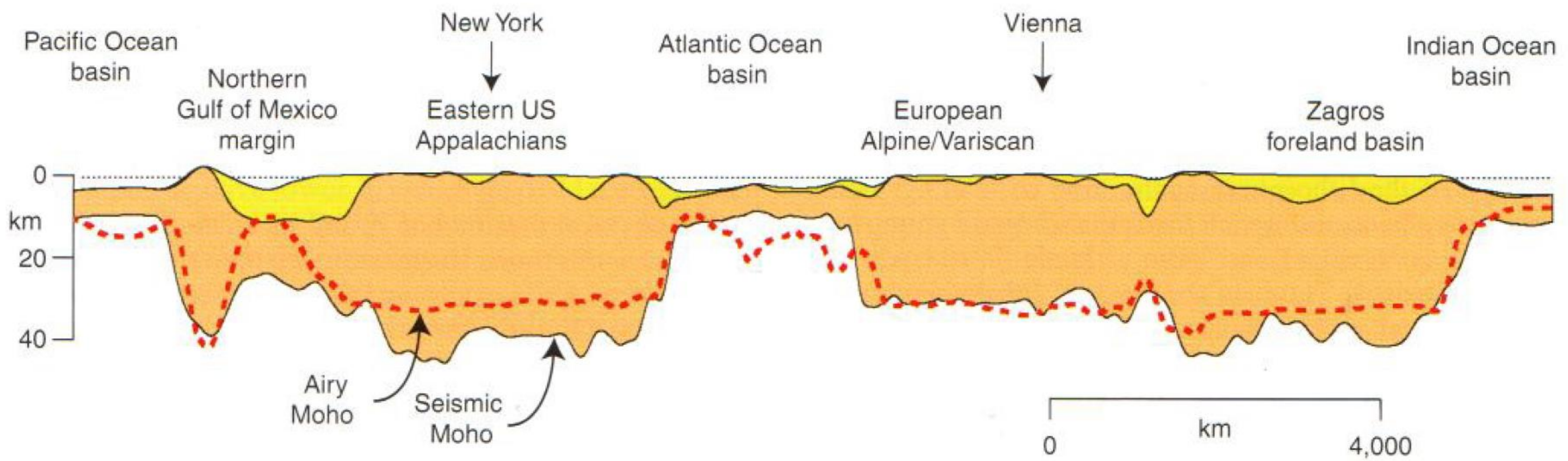

Isostasy, Figure 3 Comparison of the crustal structure based on seismic refraction data to the predicted crustal structure assuming an Airy model along an 18,000 km long great circle profile that extends from the Pacific Ocean in the west across the Atlantic Ocean to the Indian Ocean in the east. The seismic refraction data is based on CRUST2.0 http://igppweb.ucsd.edu/~gabi/rem.html and the Airy model is based on the same parameters as assumed in Figure 2.

Encyclopedia of Solid Earth Geophysics

<u>Departures to isostasy</u>:

- *Support by bending of the lithosphere for smaller-scale loads*
- *Dynamic support*

At the longest wavelengths:
deeper mass sources in a dynamic Earth

• At the global scale the near-surface isostatic signal tends to be masked by the moving, deeper mass anomalies in a convecting mantle

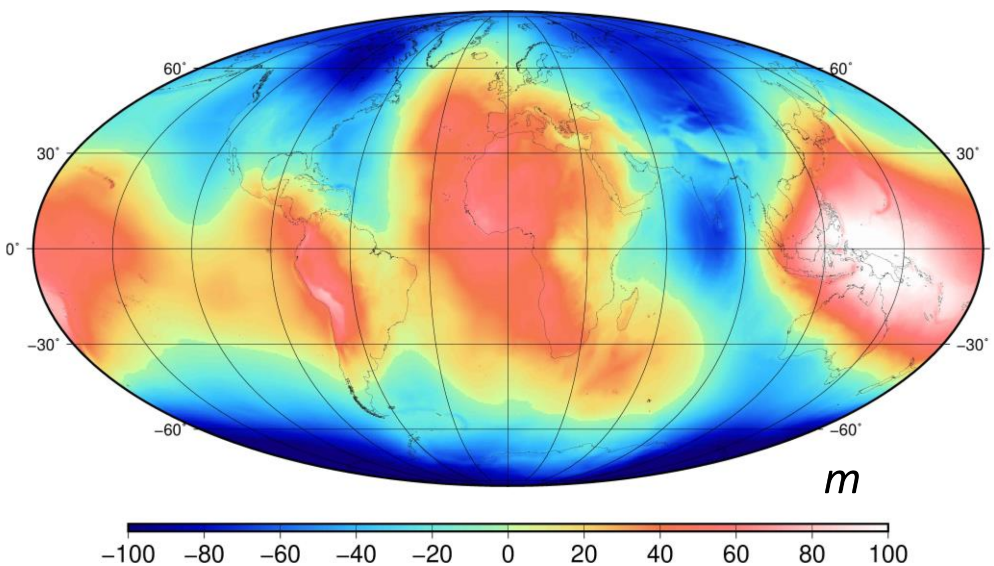

Observed geoid

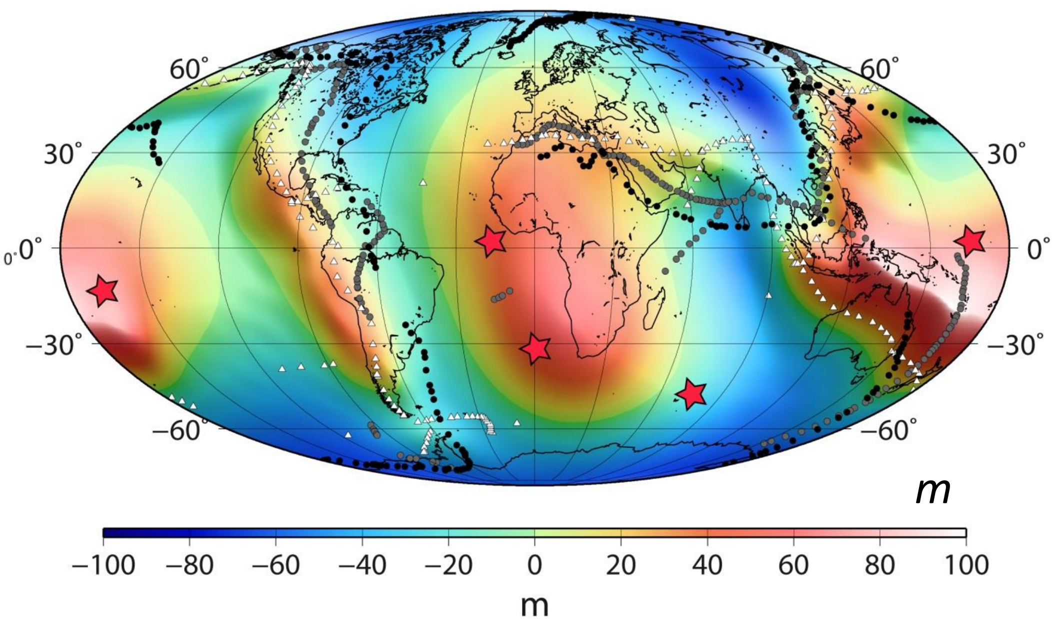

Modelled geoid from 200 Myr of subduction history and convective instabilities (Rouby et al., 2010)

See Ricard et al. (1993)

Géoïde

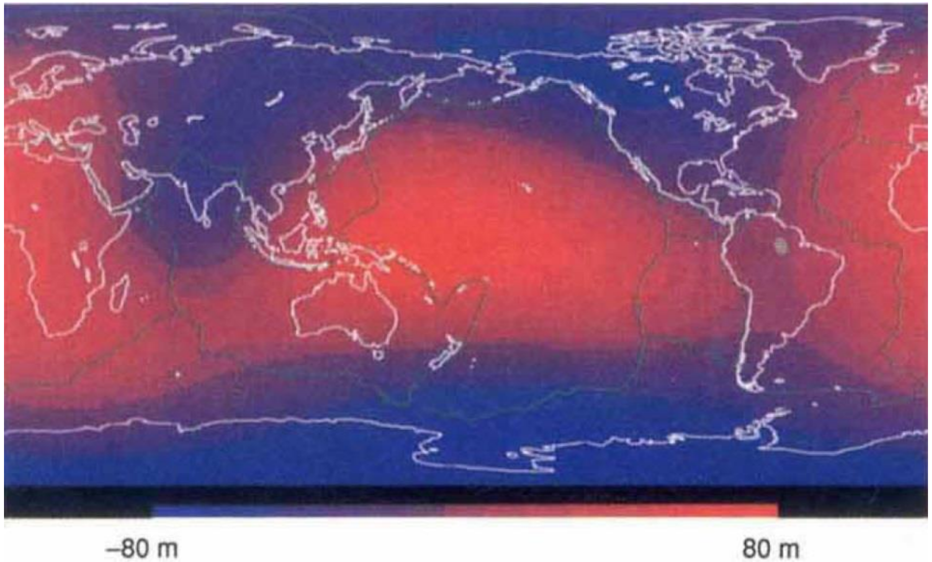

dVs

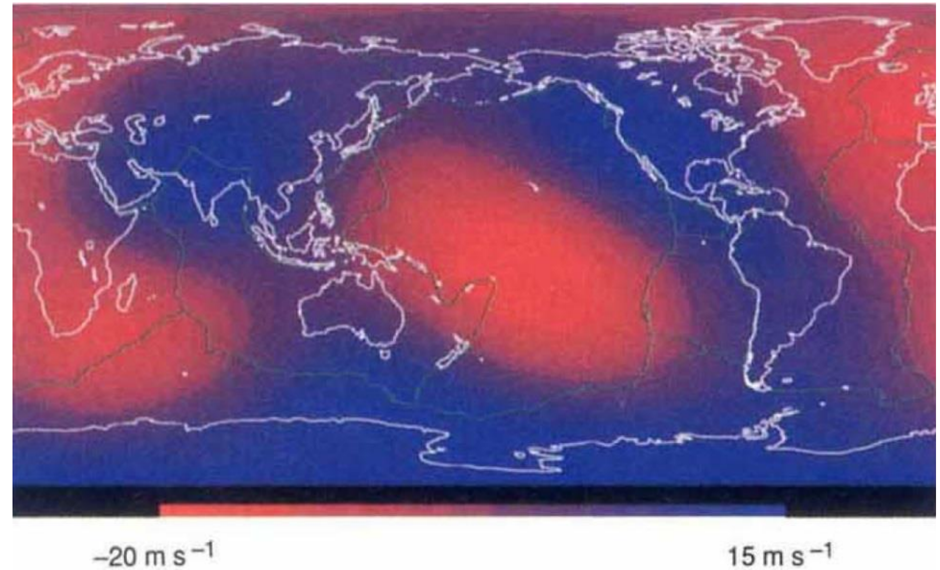

Former subduction belt

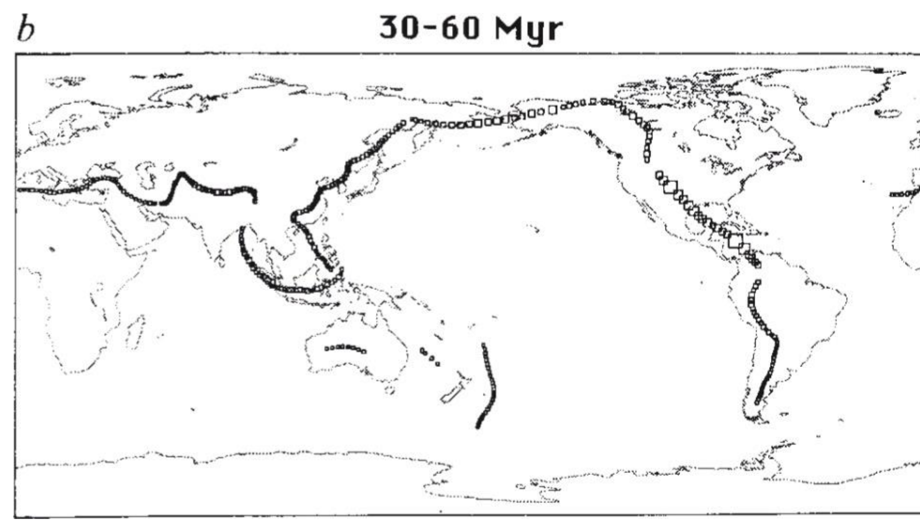

Richards & Engebretson (1992)

***Coincidence between**:*

- *Global geoid lows*
- *Fast velocities in the lower mantle* (*Dziewonski et al., 1977*)
- *Former subduction boundaries*

Moving mass anomalies in a dynamic Earth

- The flows induced by the moving mass anomaly deflect the density interfaces.

- The gravitational signal of the moving source can be counterbalanced by that of the deflected interfaces.

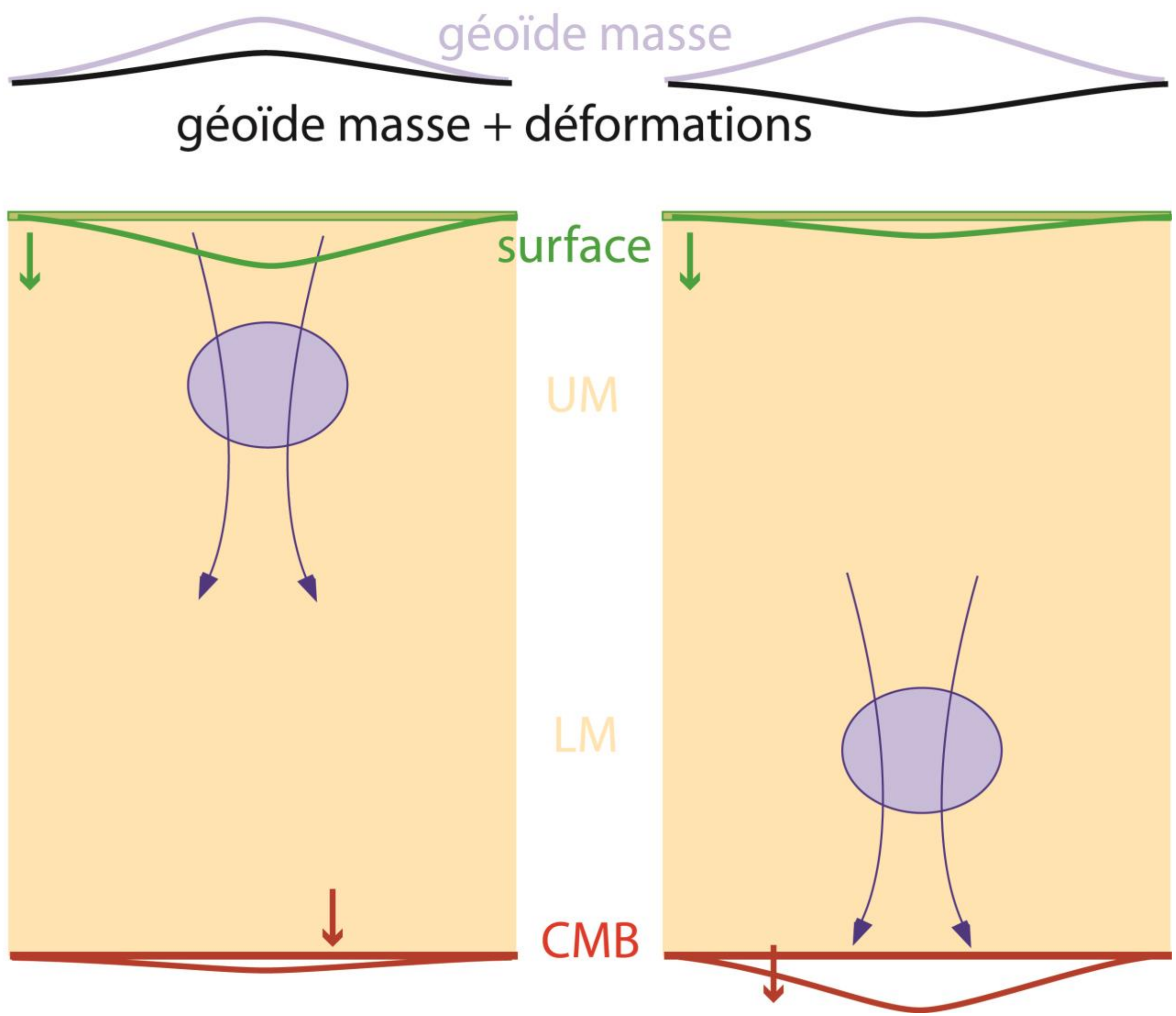

Geoid response functions

• We relate point loads (density anomalies) at each depth to the surface geoid and topography changes using wavelength-dependent response functions (= kernels defined for each spherical harmonics degree).

• These kernels are obtained by solving the system of equations that describe the Earth's viscous flow response to an internal load, in spherical geometry: conservation of mass and momentum, Poisson equation, stress-strain relation.

• Geoid kernel $G_\ell(\eta, r)$:

$$\delta N_\ell^m = \frac{3}{(2\ell+1)\bar{\rho}} \int_{r_{CMB}}^{R} G_\ell(\eta, r)\, \delta\rho_\ell^m(r) dr$$

Spherical harmonics coefficients of the non-hydrostatic geoid

Earth mean density

Mean CMB and surface radii

Spherical harmonics coefficients of the density anomalies at depth

The kernel depends on the radial mantle viscosity profile $\eta(r)$.

• Dynamic topography kernels are also defined in a similar fashion.

Richards & Hager (1984) ; Ricard et al. (1984)

Geoid response functions

1. Uniform viscosity

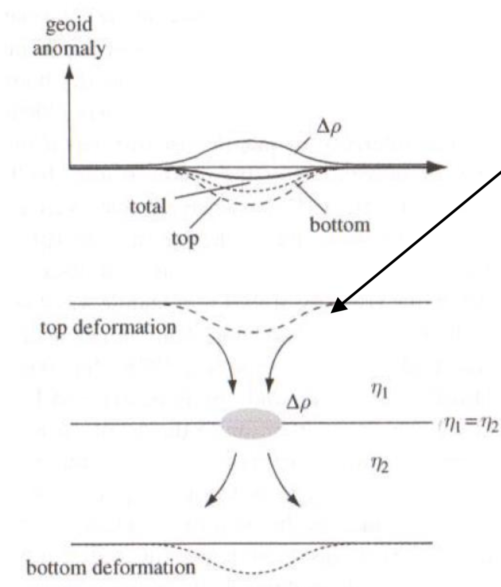

Predominant contribution → geoid low

2. Viscosity increase in the lower mantle

Predominant contribution → geoid high

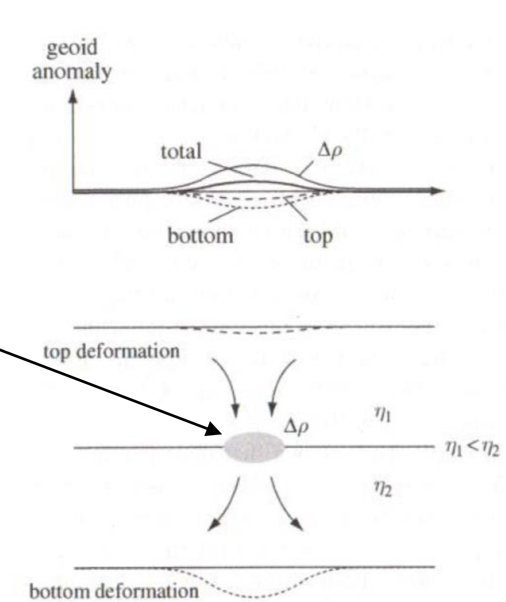

Global scale, deep source: predominant CMB contribution → geoid low

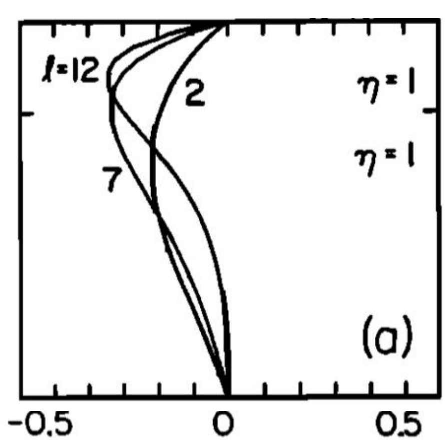

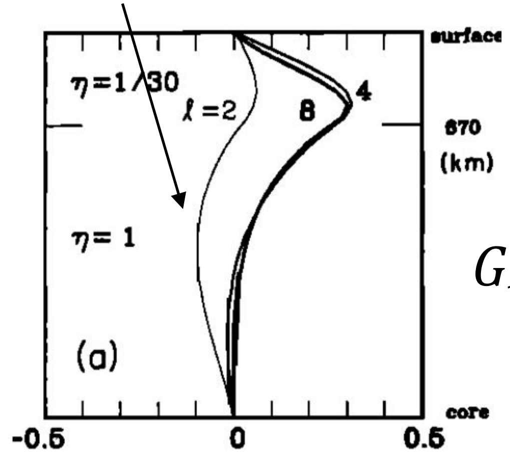

$G_\ell(\eta, r)$

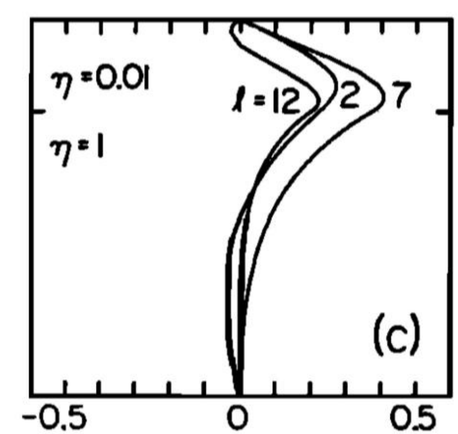

Hager (1984) – kernels for whole mantle flow ; top figures redrawn in Karato (2008).

Geometry of the sources: gravity as a vector

- Emphasize the geometry of the gravity signals
- Directional differentiations of the gravity potential T / vector $\vec{g}$

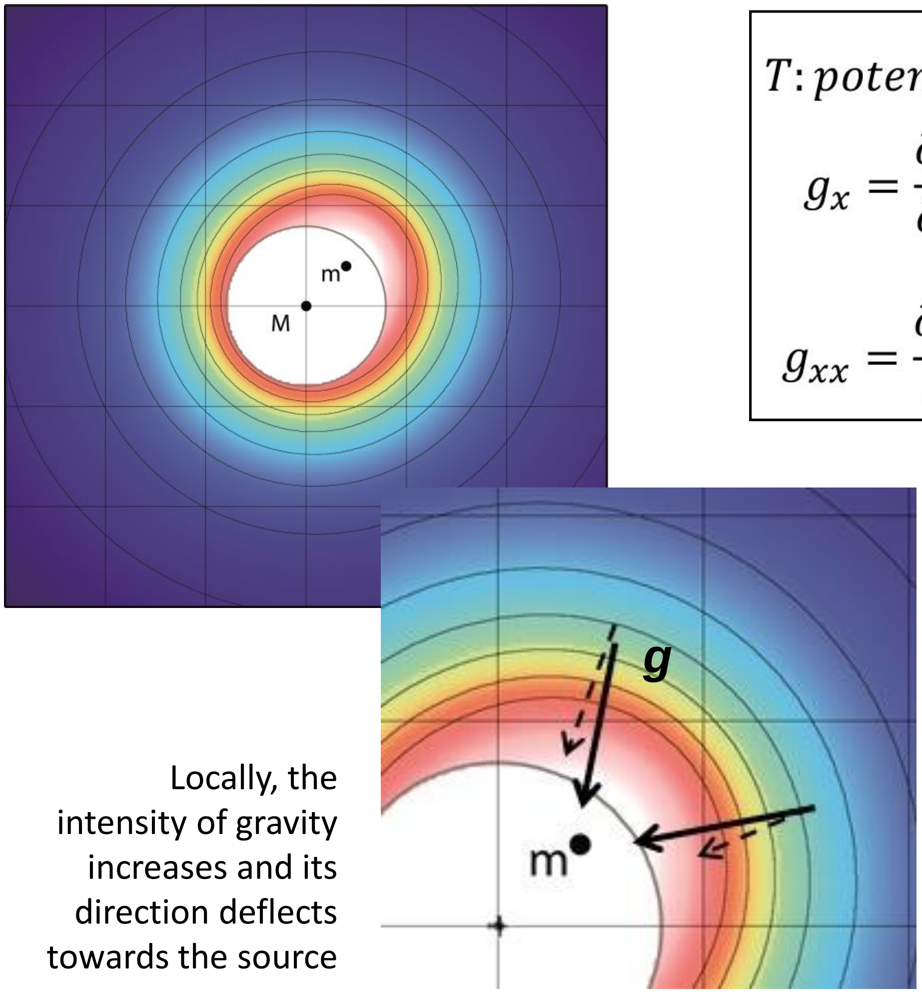

T: *potential*

$$g_x = \frac{\partial T}{\partial x}$$

$$g_{xx} = \frac{\partial g_x}{\partial x}$$

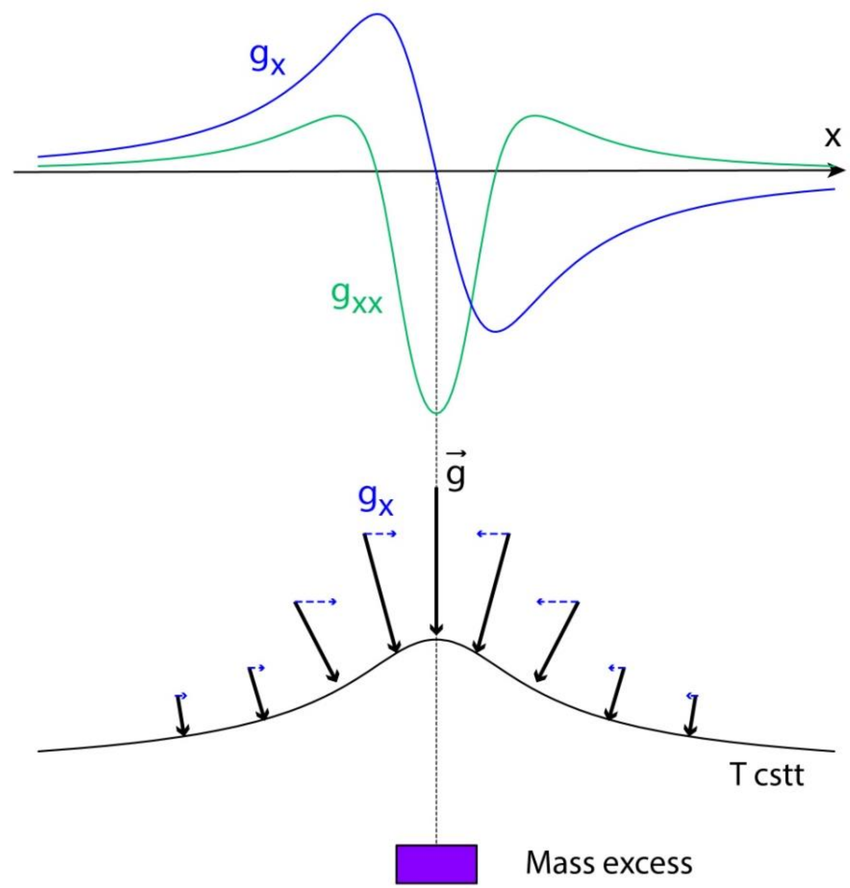

Locally, the intensity of gravity increases and its direction deflects towards the source

Example

- *Parallelepipede mass anomaly at depth w/2 - w*

- *Spherical frame*

→ Enhance gravity variations in the direction orthogonal to that of the differentiation

→ Geometry of geoid signal

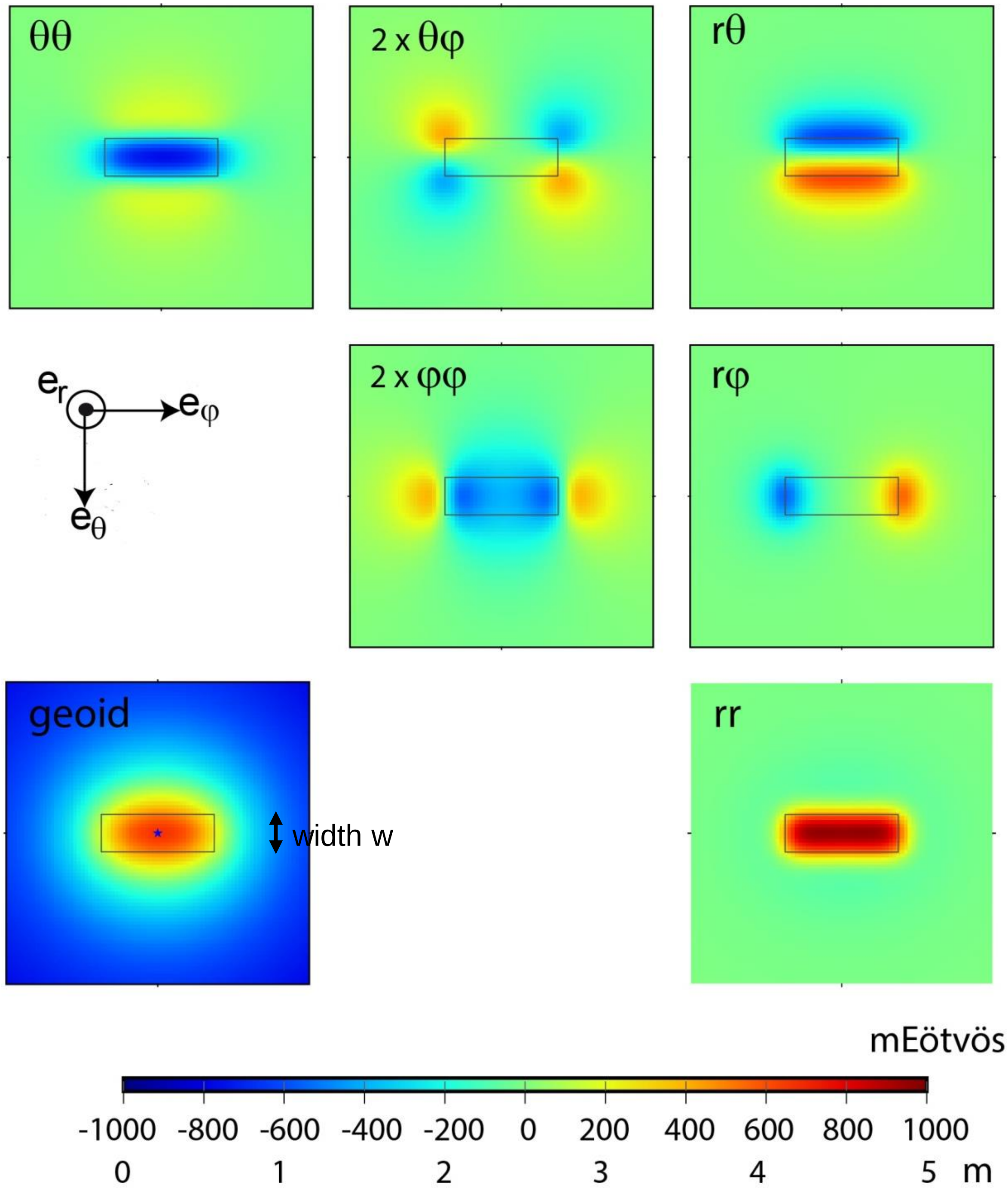

The GOCE mission

ESA, 2009-2013

Original objectives:

high resolution geoid to determine ocean currents and study the lithosphere

$$V_{ij} = \frac{\partial^2 V}{\partial x_i \partial x_j}$$

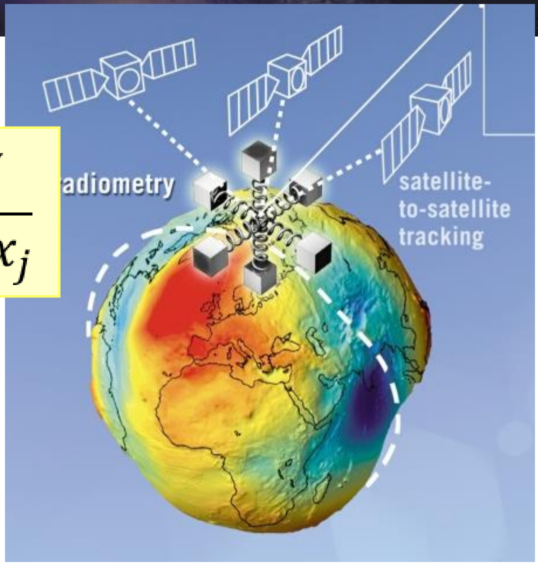

Gravity gradients from:

- a low orbit (250 km)
- gradiometry at scales < 750-1000 km
- compensation of atmospheric drag

Geometry of the mass sources

A sharper view on regional subduction patterns

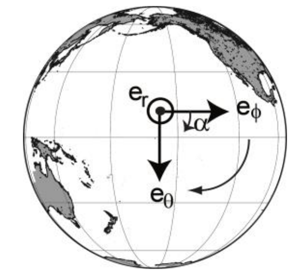

Gravity gradient signals @ GOCE altitude from:

North-South oriented masses

East-West oriented masses

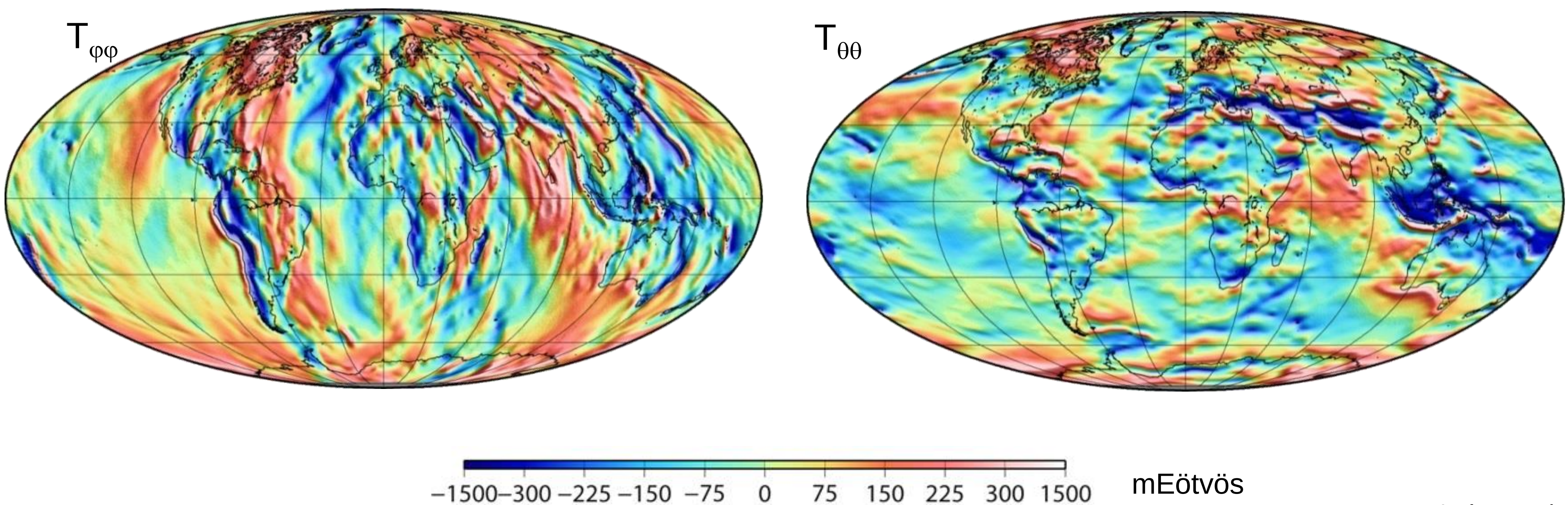

Panet et al. (2014)

- Sinking slabs → high rates of gravity variations in the East-West / North-South directions.

Curvature of the geoid from the gravity gradients

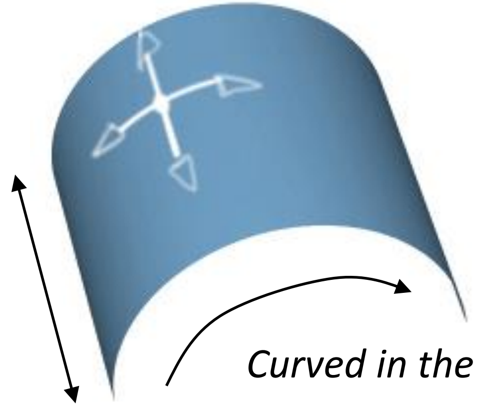

Curved in the x direction

Flat in the y direction

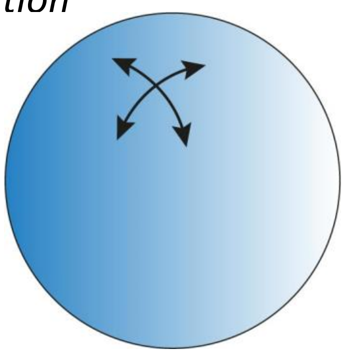

Positive curvature in the two directions

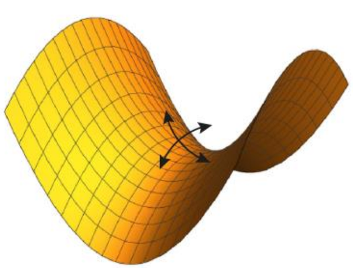

Curvatures of opposite signs in the two directions

Curvature describes how much a surface deviates from being flat. It characterizes the local shape of the surface.

The local curvature of the geoid can be computed from the gravity gradient. A shape index is defined using the maximum and minimum curvatures.

Shape Index from GOCE gradients

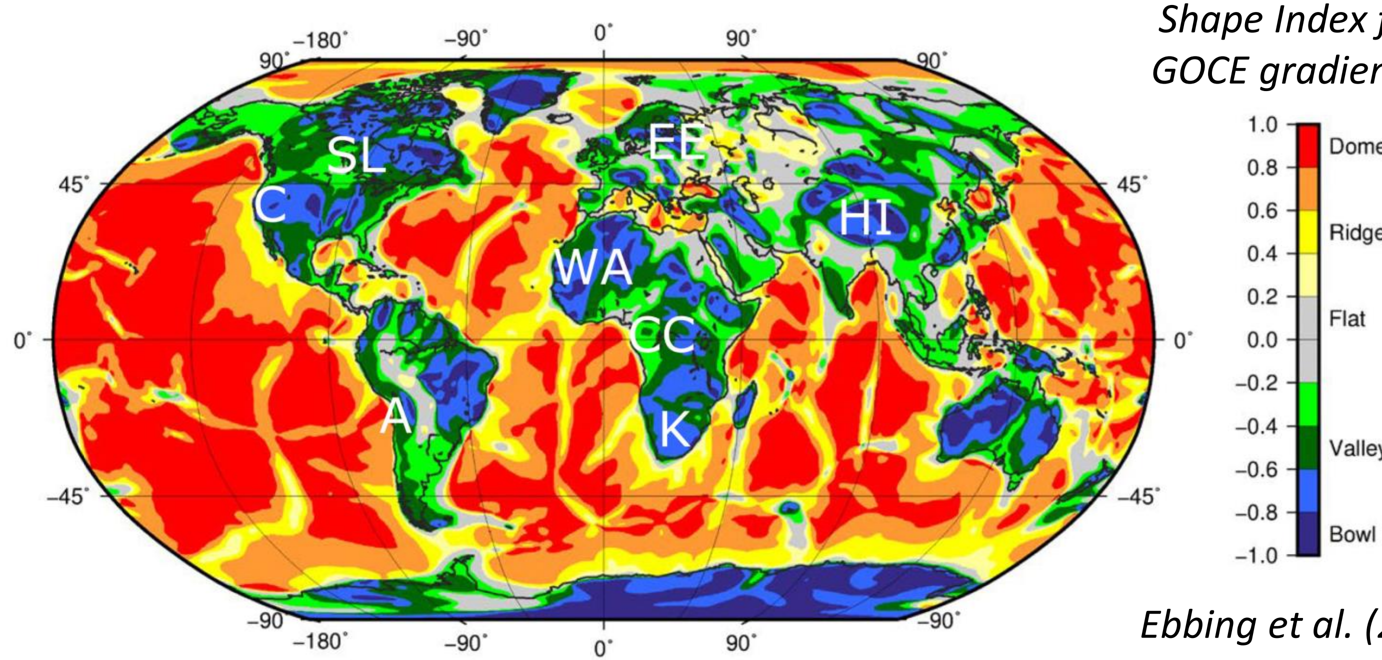

Ebbing et al. (2018)

Bowl-shaped mass default: cratonic areas, orogenic belts

The shape index varies between different cratons: interpreted as compositional variations in the crust / uppermost mantle.

Introduction to geodesy

1. A very old question: what is the shape of the Earth?

2. The revolution of the satellites

3. Gravity field from a static mass distribution and its spherical harmonics representation

4. Sources of the gravity field (geological timescales)

5. Time-varying gravity and surface displacements (timescales of weeks to secular)

$g = 9.8142627..... \ m/s^2$

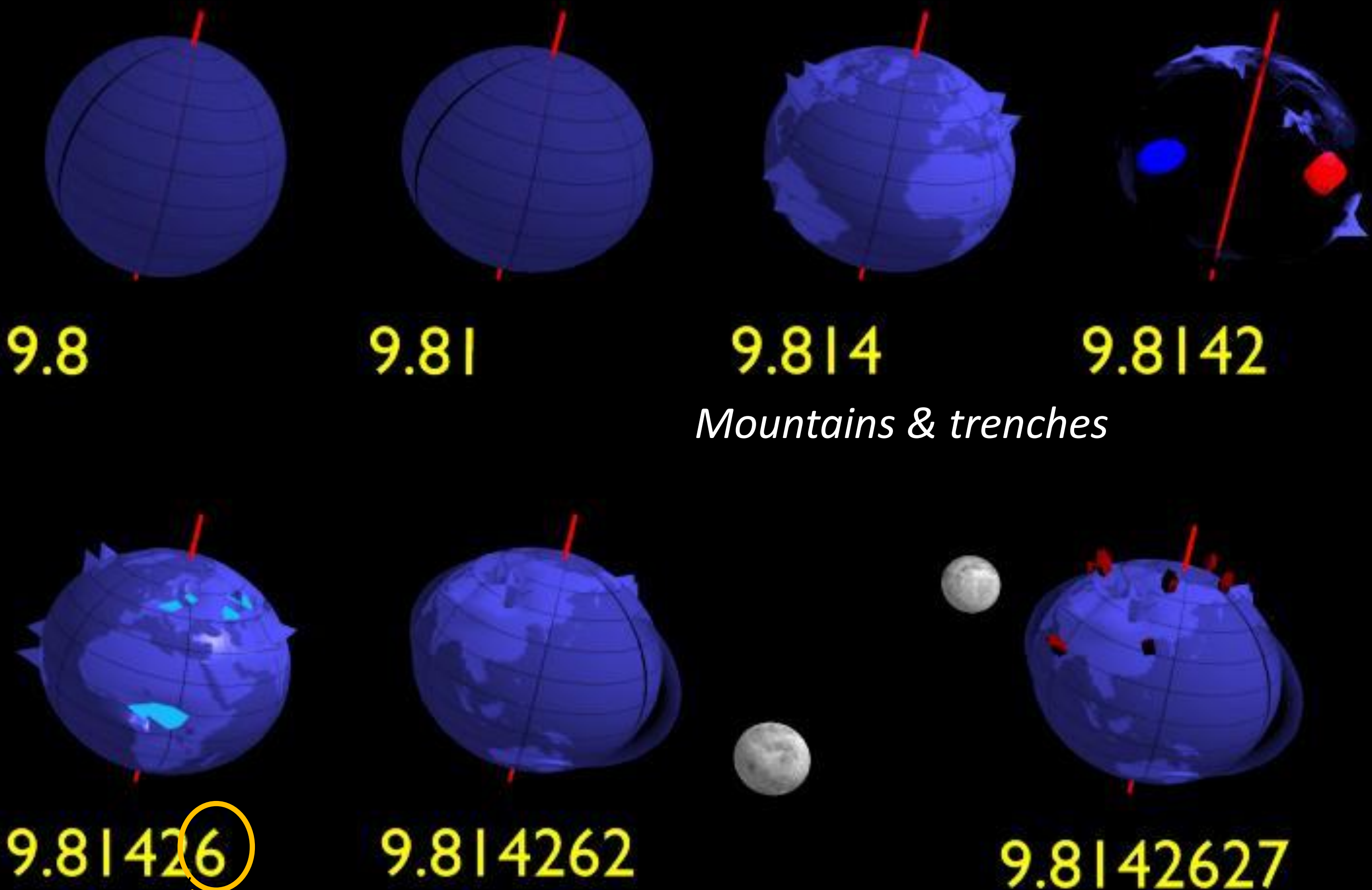

Figure: Olivier de Viron

Earth’s surface deformations

- ***Tides***: - Earth’s tides (≤ 50 cm, daily)
  - Oceanic tides (≤ 15 cm, daily)

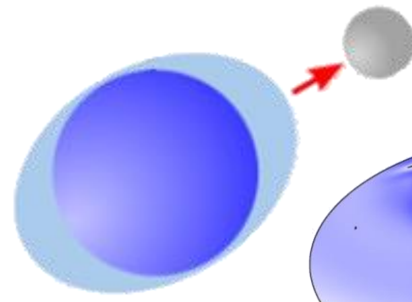

- ***Variations in flattening***

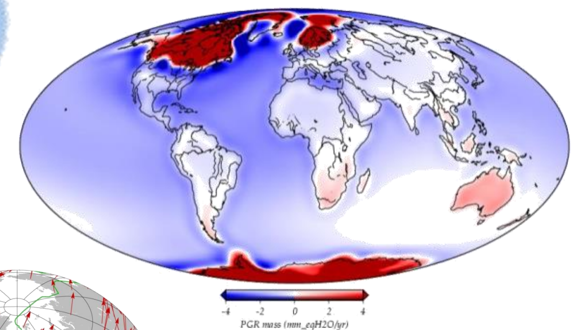

Paulson et al. (2007)

- ***Signals with large horizontal displacements***
  - Plates tectonics: mm/yr → 10 cm/yr
  - Active seismic zones

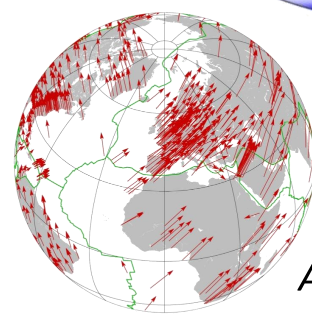

ITRF2014
Altamimi et al.

- ***Signals with significant vertical displacements***
  - Response to surface water loads at different timescales
    - atmosphere, hydrology, cryosphere, oceans: cm
    - post-glacial rebound (secular: mm/yr)

- Earthquakes, volcanoes
- Pumping

Loading signals also in the horizontal motions

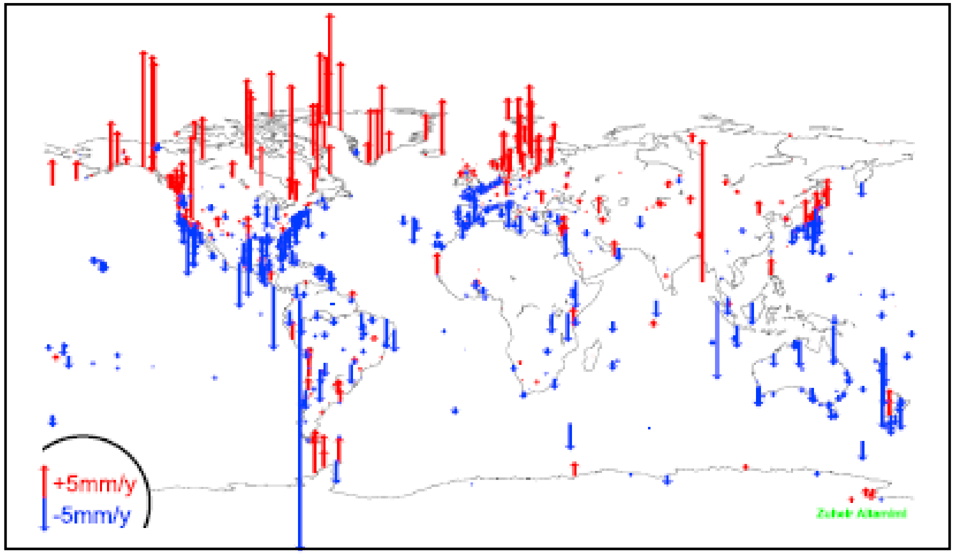

Vertical velocities

ITRF2014, Altamimi et al.

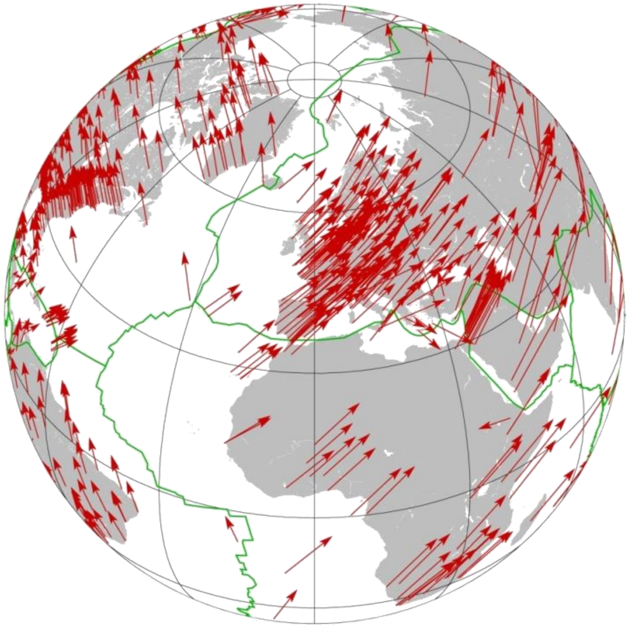

Horizontal velocities

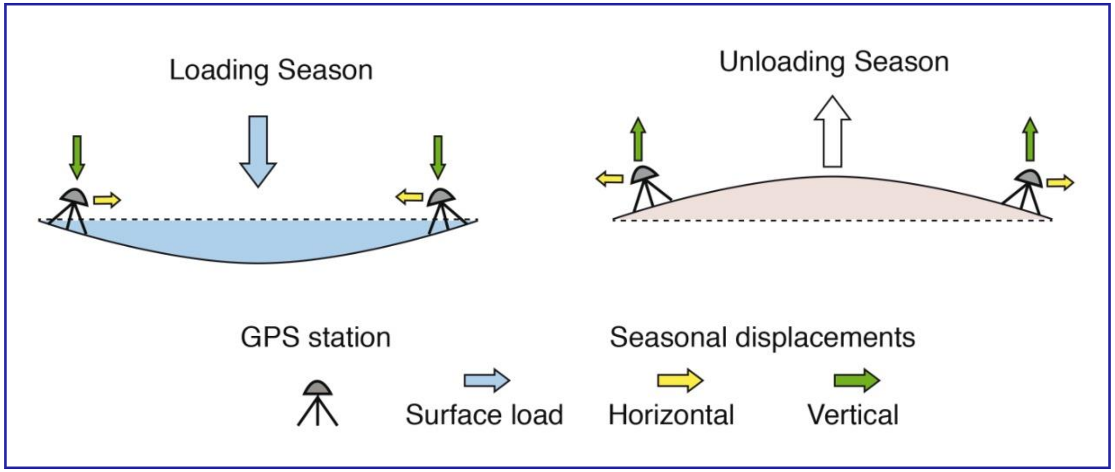

Courtesy of Kristel Chanard

Time-varying gravity & the GRACE mission

Add altitude, 220 km dist

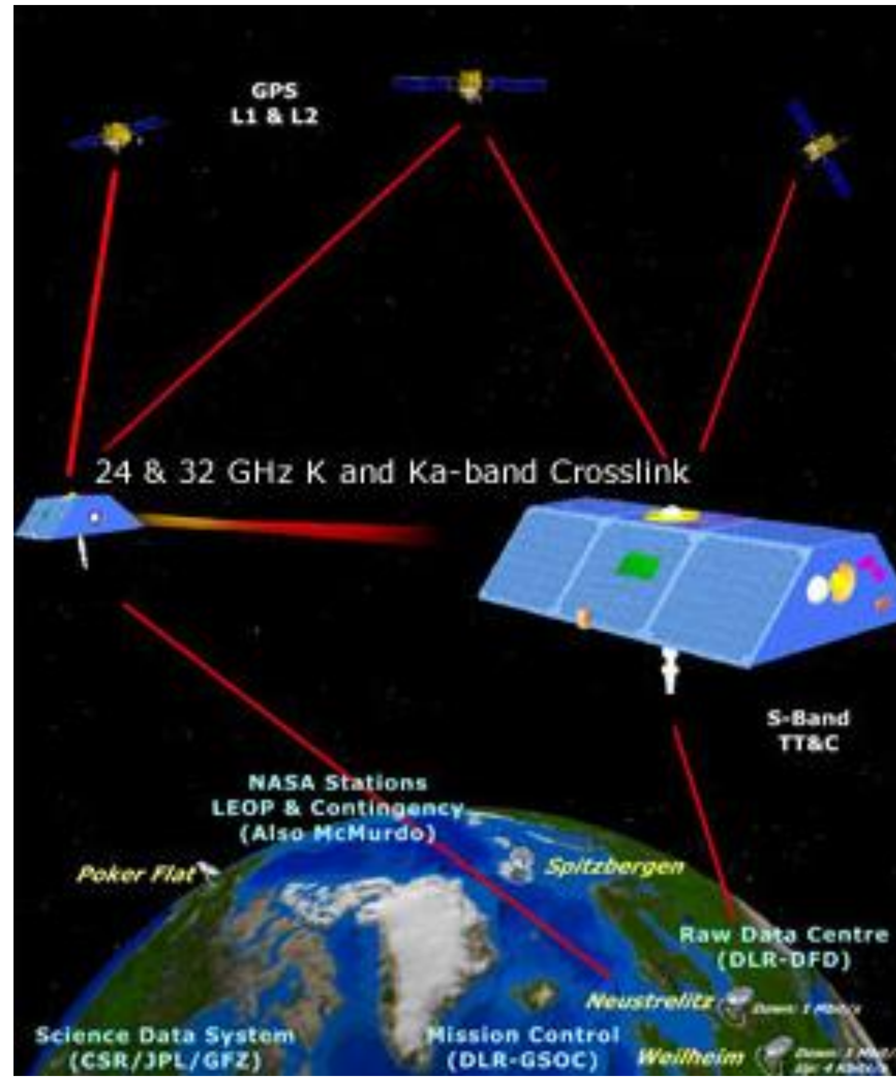

- Two satellites following each other on the same orbit

- Measurement of the inter-satellites distance / relative velocity (accuracies: 10 μm / few μm/s) from a microwave signal emitted by one satellite and reflected by the other.

- Non-gravitational forces measured by ONERA accelerometers (accuracy: 10^{-10} m/s^2)

Principle

Effect of a local mass excess source on the distance between the two GRACE satellites ?

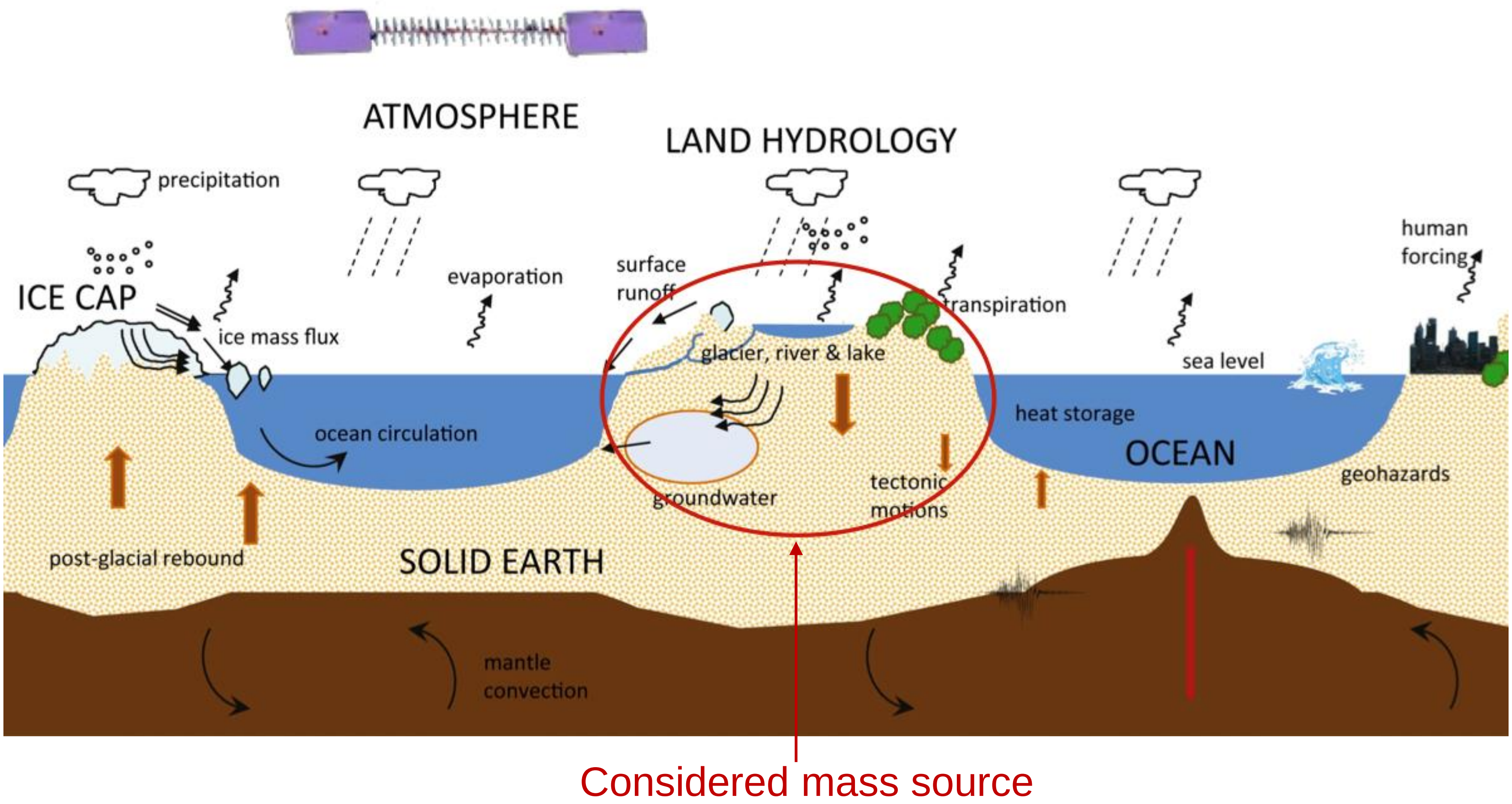

Principle

Satellite 2 not accelerated because its distance to the mass source is large

Inter-distance increases

Satellite 1 accelerates because its distance to the mass source decreases

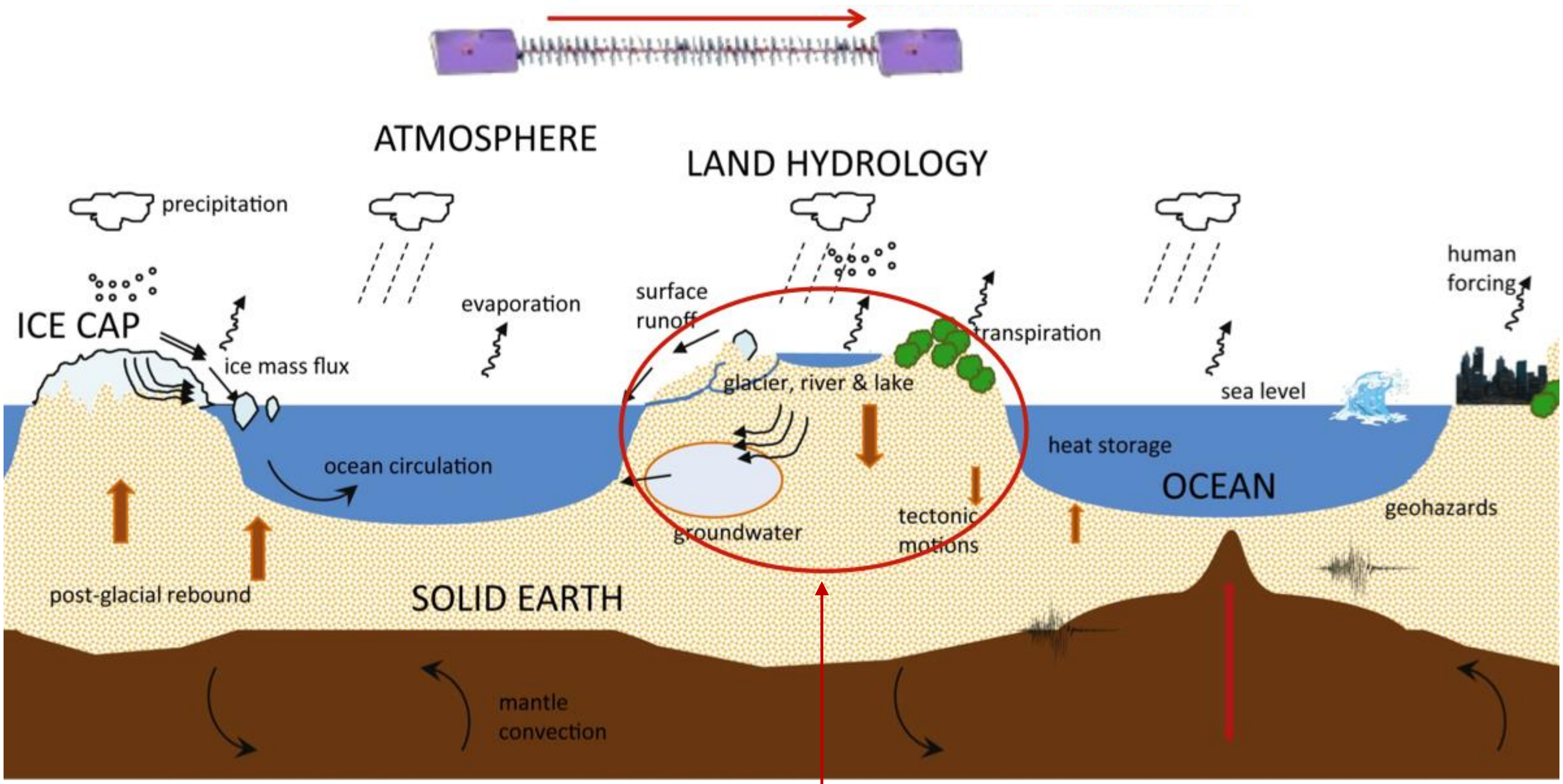

Considered mass source

Principle

Satellite 2 accelerates because its distance to the mass source decreases

Inter-distance decreases

Satellite 1 decelerates because its distance to the mass source increases

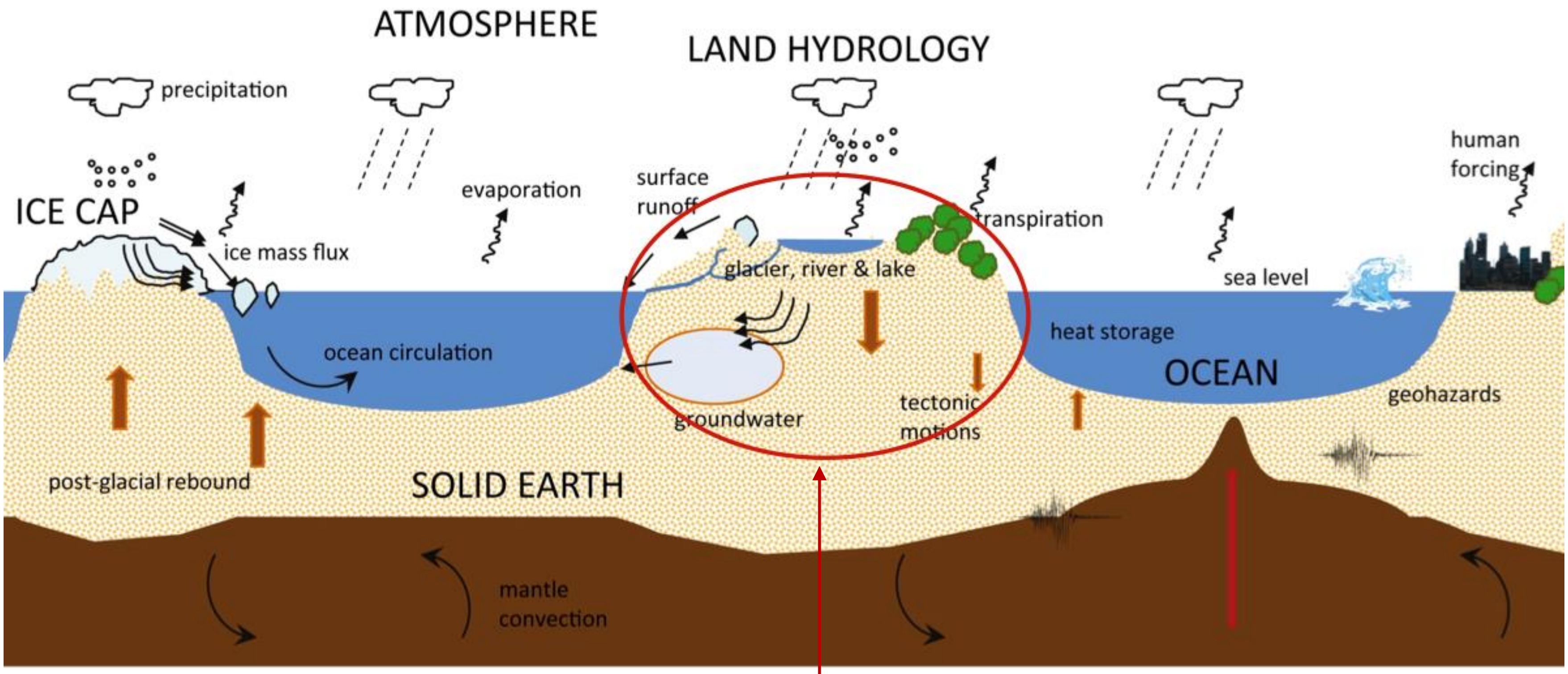

Considered mass source

Monthly spherical harmonics models of the geoid

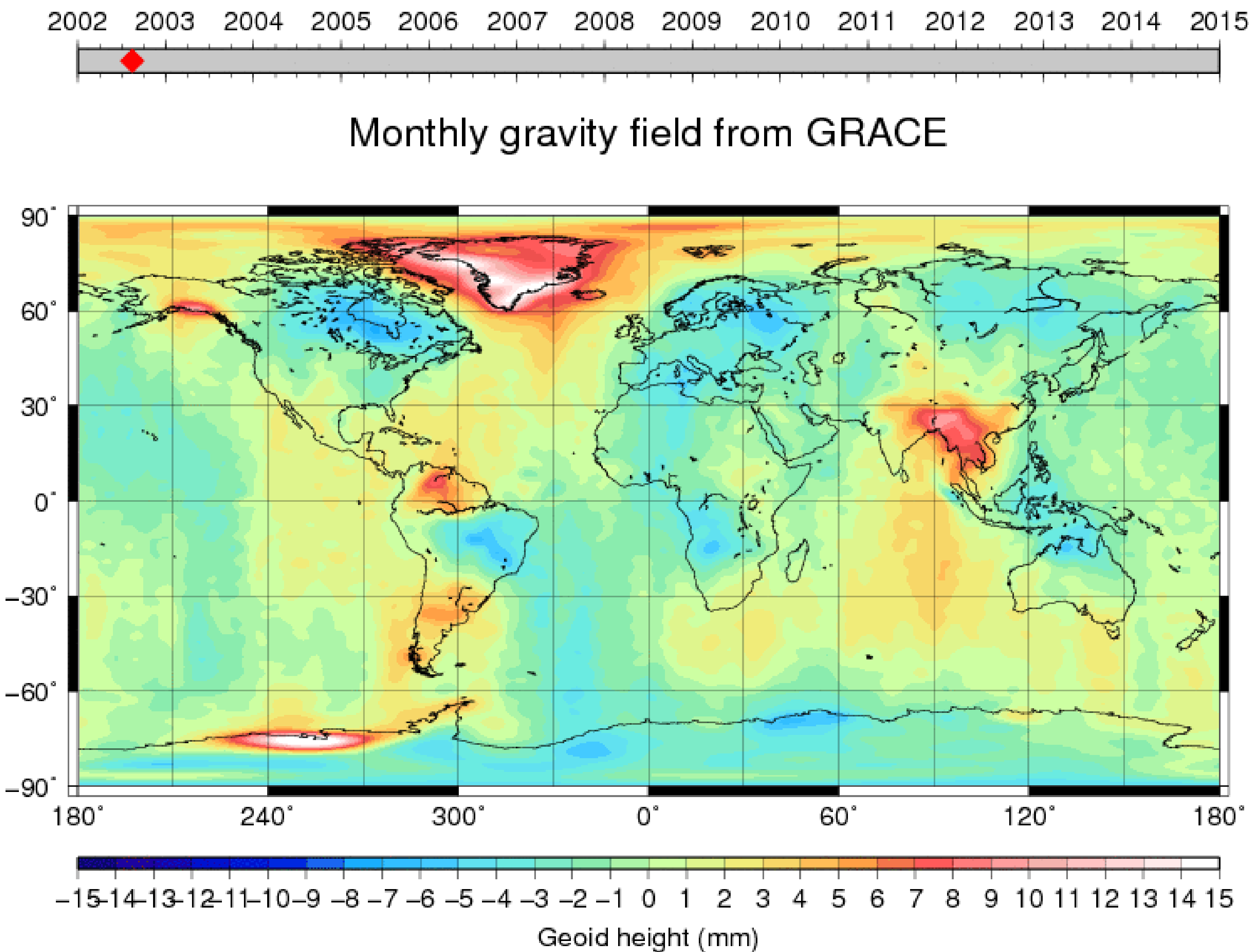

R.Biancale, J-M. Lemoine et al. (2014)

Thin layer potential

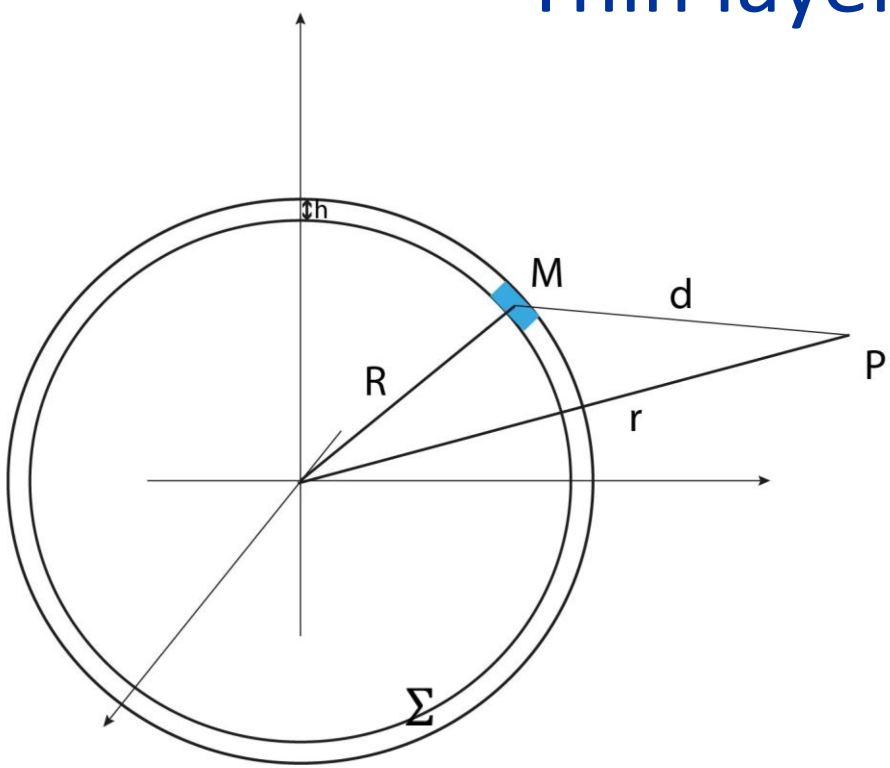

- Surface load σ in M:

$$\sigma(\theta,\varphi) = \sum_{\ell=0}^{\infty}\sum_{m=-\ell}^{\ell}\sigma_{\ell,m}Y_\ell^m\,(\theta,\varphi)$$

$$\sigma(\theta,\varphi) = \sum_{\ell=0}^{\infty}\sigma_\ell\,(\theta,\varphi)$$

- Its potential in P:

$$W(\theta_P,\varphi_P) = \int_\Sigma \frac{\sigma(\theta,\varphi)}{d}\,d\sigma(\theta,\varphi) \qquad (1)$$

- In (1) we introduce the development of 1/d (see slide X) and that of σ:

$$W(r_P,\theta_P,\varphi_P) = \sum_{\ell=0}^{\infty}\sum_{m=-\ell}^{\ell}\left(\frac{R}{r_P}\right)^{\ell+1}\frac{4\pi GR}{2\ell+1}\,\sigma_{\ell,m}\,Y_\ell^m(\theta_P,\varphi_P)$$

- At the surface: $W(\theta,\varphi) = \frac{3g_0}{\rho}\sum_{\ell=0}^{\infty}\frac{\sigma_\ell(\theta,\varphi)}{2\ell+1} = \sum_{\ell=0}^{\infty}W_\ell(\theta,\varphi)$

$g_0 = \frac{GM}{R^2}$; $M = \frac{4}{3}\pi R^3\rho$; $\rho = 5520$ kg/m³

Validity: Wahr et al 1998

$$\left(\frac{R}{R+h}\right)^{\ell+2} \sim 1$$

$$(\ell_{max}+2)\frac{h}{R} \ll 1$$

Earth's deformations under a surface load

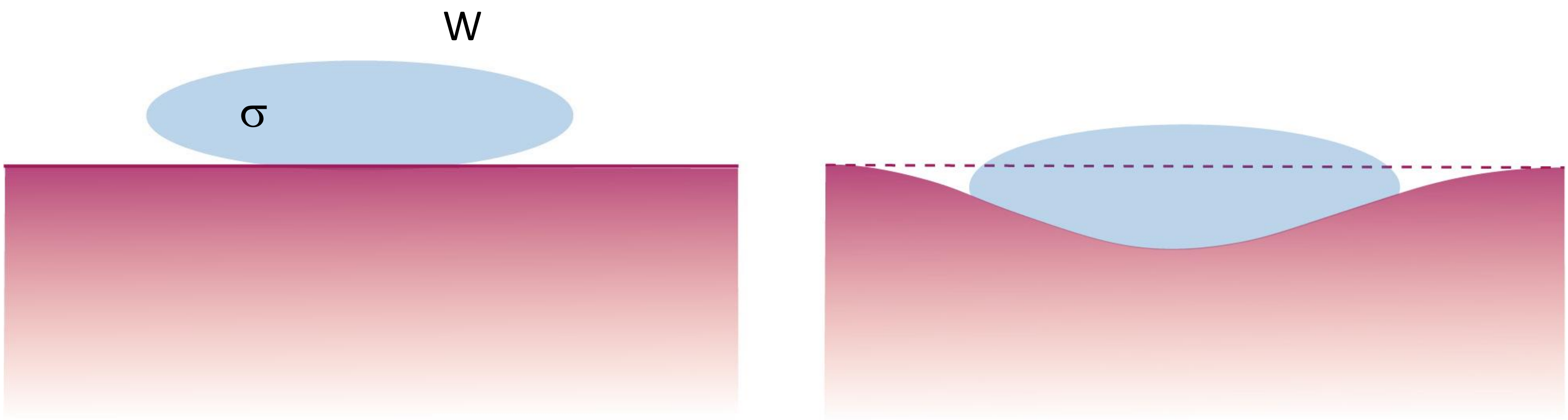

W: gravitational potential of the mass load

V: gravitational potential associated with the deformations within the Earth caused by the mass load (surface displacements (u_v, u_h) + internal mass redistribution)

$$V = k'W \quad ; \quad u_r = h'\frac{W}{g_0} \quad ; \quad u_\theta = \frac{\ell'}{g_0}\frac{\partial W}{\partial \theta} \quad ; \quad u_\varphi = \frac{\ell'}{g_0}\frac{1}{\sin\theta}\frac{\partial W}{\partial \varphi}$$

co-latitude *longitude*

k', *h'*, *l'* are dimensionless **load Love numbers** (Love, 1909).

Actually, they depend on the spherical harmonics degree. They depend on time in the visco-elastic case.

Earth's deformations under a surface load

- **Elastic load Love numbers**: describe the response of the Earth to the body force and the surface normal traction caused by a unit mass loading. Obtained by integrating the equations of motion, the stress-strain relation and the Poisson equation for a self-gravitating spherical Earth initially at hydrostatic equilibrium (e.g. Farrell, 1972).

- For each degree, the surface deformations are proportionnal to the potential induced by the loading mass or its derivative:

$$u_r(\theta,\varphi) = \frac{3}{\rho}\sum_{n=0}^{\infty}\frac{h'_n}{2n+1}\,\sigma_n(\theta,\varphi) = \sum_{n=0}^{\infty}\frac{h'_n}{g_0}W_n(\theta,\varphi)$$

$$u_h(\theta,\varphi) = \frac{3}{\rho}\sum_{n=0}^{\infty}\frac{\ell'_n}{2n+1}\,\nabla_h\sigma_n(\theta,\varphi) = \sum_{n=0}^{\infty}\frac{\ell'_n}{g_0}\nabla_h W_n(\theta,\varphi)$$

horizontal displacement

- Perturbation of the gravity potential:

$$\delta V(\theta,\varphi) = \frac{3}{\rho}\sum_{n=0}^{\infty}\frac{k'_n}{2n+1}\,\sigma_n(\theta,\varphi) = \sum_{n=0}^{\infty}\frac{k'_n}{g_0}W_n(\theta,\varphi)$$

- Total variation of the gravity potential (at a fixed point, not on the moving surface):

$$V(\theta,\varphi) = \frac{3}{\rho}\sum_{n=0}^{\infty}\frac{1+k'_n}{2n+1}\,\sigma_n(\theta,\varphi)$$

- **Visco-elastic case**: the Love numbers depend on the temporal frequency of excitation.

Examples: monitoring of aquifers depletion

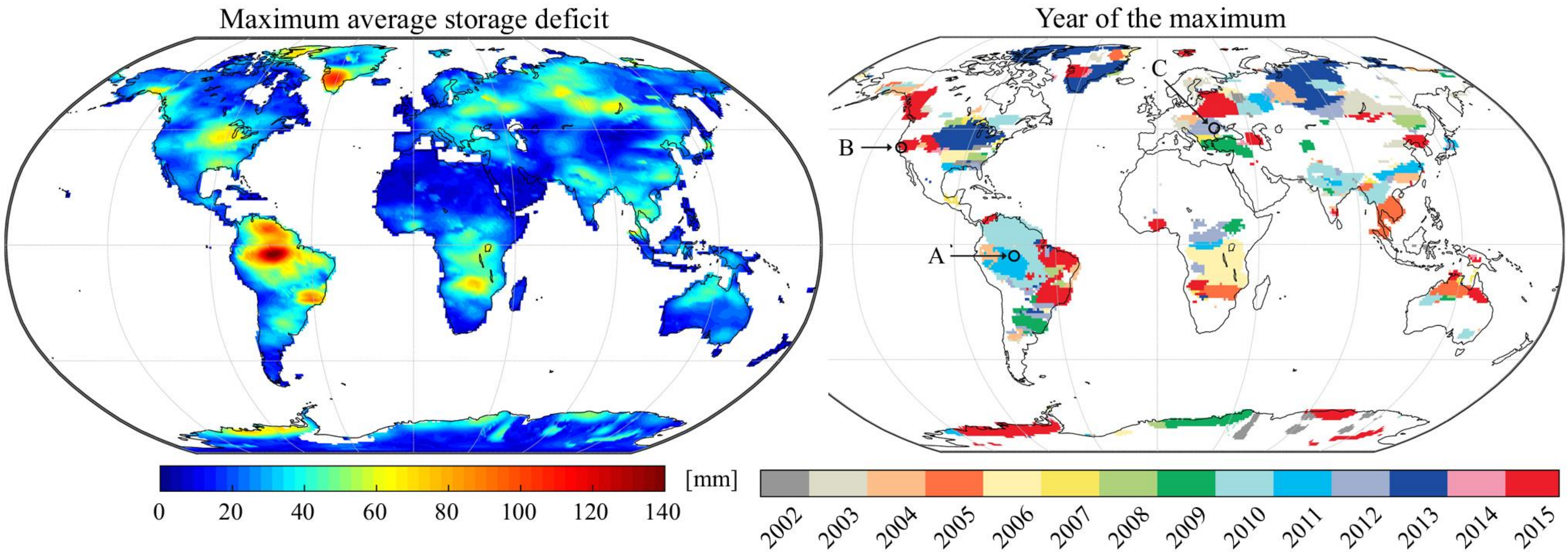

Humphrey et al. (2016)

4D space-time monitoring of water transport

Homogeneous space-time coverage from satellites

Earth's response to seasonal hydrology

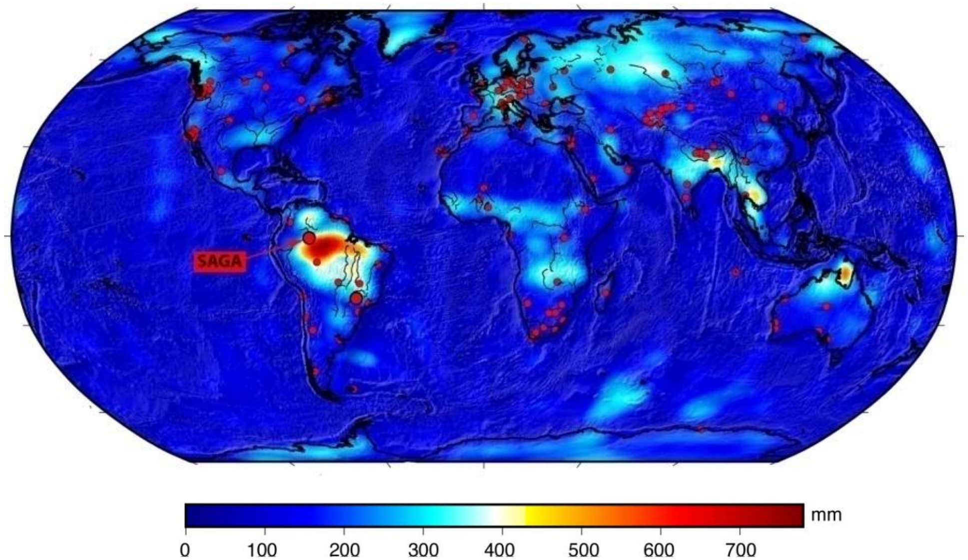

Seasonal water load from GRACE gravity

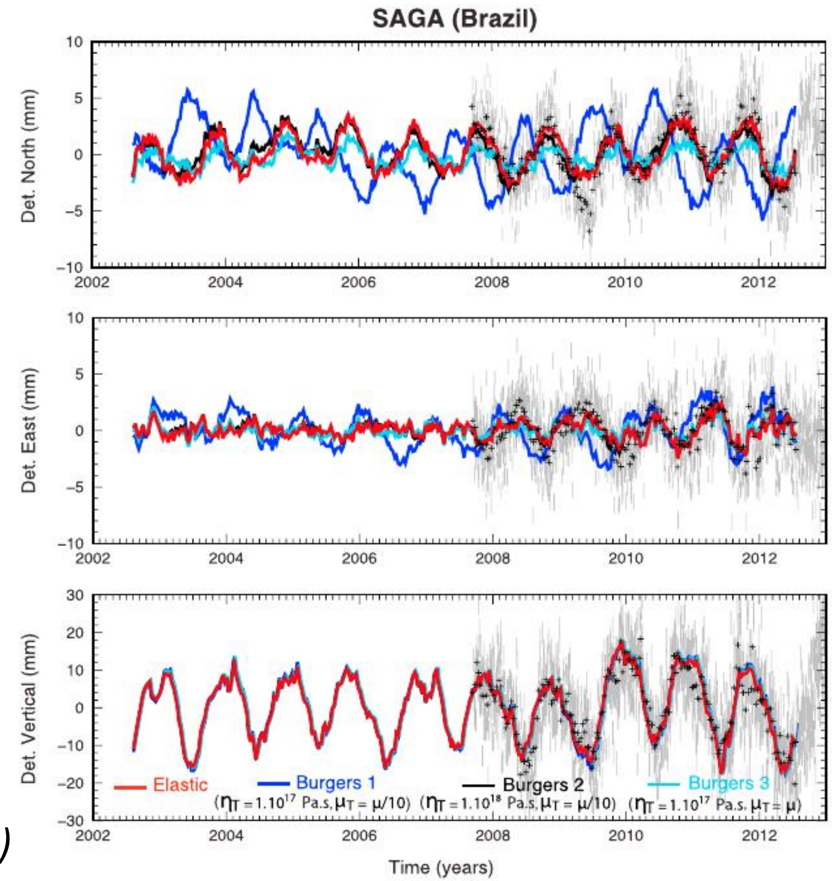

Chanard et al. (2018)

• Testing different asthenospheric rheologies to predict the surface displacements under a seasonal hydrological load & comparison with GPS.

• Transient asthenospheric viscosity should not be lower than 5 10^{17} Pa.s to explain the horizontal displacement induced by seasonal water loads, in global average.

Thank you!